



This is to certify that the
thesis entitled
Computer Modeling and Evaluation of a
Cometabolic Sequencing Batch Reactor

presented by
Robert A. Solak Jr.

has been accepted towards fulfillment
of the requirements for

M.S. degree in Environmental
Engineering


Major professor

Date 3/27/98

LIBRARY
Michigan State
University

PLACE IN RETURN BOX
to remove this checkout from your record.
TO AVOID FINES return on or before date due.

DATE DUE	DATE DUE	DATE DUE
120902 DEC 13 2001		

**COMPUTER MODELING AND EVALUATION OF A COMETABOLIC
SEQUENCING BATCH REACTOR**

By

Robert A. Solak Jr.

A THESIS

**Submitted to
Michigan State University
in partial fulfillment of the requirements
for the degree of**

MASTER OF SCIENCE

Department of Civil and Environmental Engineering

1998

ABSTRACT

COMPUTER MODELING AND EVALUATION OF A COMETABOLIC SEQUENCING BATCH REACTOR

By

Robert A. Solak Jr.

Trichloroethylene, a common industrial solvent and pollutant, has been demonstrated to be degradable by cometabolism using phenol as a growth substrate. Competitive inhibition for oxygenase enzymes has created problems in implementing cometabolism as a treatment alternative for trichloroethylene. Intermittent feeding strategies, with separate time periods for consumption of the two substrates, have been developed to avoid such problems. Sequencing batch reactors are one system capable of separating periods of substrate consumption.

In this study, a model of an aerobic sequencing batch reactor is developed and modeled by computer. Predictions of substrate concentrations, biomass concentrations, and the mass of trichloroethylene lost to air stripping are compared to observations made from laboratory scale reactors. Parameters used in the model are determined by independent experiments. A sensitivity analysis is also performed on the model to determine the relative importance of various parameters to model predictions.

**Dedicated to all those graduate students
who have seen deadlines come,
and deadlines go...**

ACKNOWLEDGEMENTS

I would like to offer many thanks to my advisor, Dr. Craig Criddle, who had an answer for every question and suggestions for every problem.

I would also like to thank my committee members, Dr. David Wiggert and Dr. Robert Hickey for their comments and suggestions as well as Wang-Kwan Chang and Stephen Callister for their tireless efforts to maintain and care for the reactors that I merely “borrowed” on occasion. To Stephen, I owe a special thanks for running phenol samples and lending some data when I needed it.

To my parents I am eternally grateful for all they did to give me my opportunities in life. To my siblings and siblings-in-law, I thank them for their unending question “Is your thesis done yet?”. And lastly, I will always be thankful to my wife for all the love, companionship and support she gave me as I did what I had to do.

TABLE OF CONTENTS

LIST OF TABLES.....	vii
LIST OF FIGURES.....	viii
NOMENCLATURE.....	ix
CHAPTER 1 INTRODUCTION	1
CHAPTER 2 MODEL DEVELOPMENT	5
Phenol Degradation	5
TCE Degradation.....	9
Mass Balance Equations	11
CHAPTER 3 MATERIALS AND METHODS.....	17
Reactor Design and Maintenance	17
Initial Degradation Rate Studies.....	18
Measurement of Volatile TCE Loss During Fill Cycle.....	20
Measurement of Liquid Phase TCE.....	20
Phenol Measurements.....	21
Kinetic Parameters.....	21
CHAPTER 4 PARAMETER DETERMINATION	26
Yield on Phenol, Y	26
Observed Specific Growth Rate of TCE-degrading Biomass, μ_{apt}	27
Endogenous Decay Coefficient, b	29
TCE-degrading Biomass Decay Coefficient, b_{apt}	29
Transformation Capacity, T_c^b	30
Zero-Order Phenol Degradation Coefficient, k^o	30
TCE First-Order Rate Coefficient, k'	31
CHAPTER 5 COMPUTER MODELING AND EXPERIMENTAL VERIFICATION	32

MathCAD Modeling.....	32
Experimental Results.....	34
One Population Model.....	37
Two Population Model	44
CHAPTER 6	
MODEL SENSITIVITY AND PARAMETER UNCERTAINTY.....	45
Relative Sensitivity.....	45
Parameter Uncertainty	48
CHAPTER 7	
CONCLUSIONS AND RECOMMENDATIONS	55
Computer Modeling.....	55
Parameter Determination.....	55
Recommendations	56
REFERENCES	58
APPENDIX A	
MATHCAD PROGRAMMING.....	60
APPENDIX B	
MASS TRANSFER COEFFICIENT DETERMINATION.....	63

LIST OF TABLES

Table 3-1 SBR Schedule and Activity.....	17
Table 3-2 Reactor Conditions.....	18
Table 3-3 Gas Chromatograph Operating Parameters.....	19
Table 4-1 Kinetic Parameters Used in Computer Modeling.....	26
Table 5-1 Solids Data.....	41
Table 6-1 Relative Sensitivity.....	48
Table A-1 MathCAD Variable Legend.....	62

LIST OF FIGURES

Figure 1-1 Oxygenase Mediated Co-metabolism.....	2
Figure 5-1 MathCAD Programming Logic	33
Figure 5-2 TCE in the Reactor.....	34
Figure 5-3 Phenol in the Reactor.....	36
Figure 5-4 Solids Concentration over Time.....	37
Figure 5-5 One-population Model Predictions.....	38
Figure 5-6 TCE Model and Data.....	40
Figure 5-7 Phenol Model and Data.....	43
Figure 6-1 Uncertainty Modeling for Yield.....	50
Figure 6-2 Uncertainty Modeling for k'	51
Figure 6-3 Uncertainty Modeling for k^o	52
Figure 6-4 Uncertainty Modeling for b	53
Figure A-1 MathCAD Programming Worksheet.....	61
Figure A-2 MathCAD Equation Matrix.....	62
Figure A-3 MathCAD Program.....	63
Figure B-1 Mass Transfer Coefficient Relationship.....	65

NOMENCLATURE

b	endogenous decay rate (1/day)
C	Non-growth substrate concentration (mg/L)
K_s	half saturation coefficient (mg/L)
k^0	zero-order rate coefficient (1/day)
μ	specific growth rate (1/day)
H	dimensionless Henry's constant
K_i	inhibition constant
k'	first-order TCE degradation rate (L/mg-day)
k	substrate utilization rate (1/day)
M	Mass (mg)
Q	liquid flowrate (L/hr)
Q_g	gaseous flowrate (L/hr)
S	Growth substrate concentration (mg/L)
t	time (days)
T_c^b	Transformation capacity (mg TCE/mg cells)
T_c^{b*}	True transformation capacity (mg TCE/mg cells)
V	liquid volume (L)
Y	yield coefficient (mg TSS/mg phenol)
X	Biomass concentration (mg/L)

subscripts

a	active organisms
p	phenol-degrading organisms
t	TCE-degrading organisms
L	liquid phase
g	gaseous phase

CHAPTER 1

INTRODUCTION

Co-metabolism is defined as the degradation of non-growth substrate by microorganisms which receive no apparent benefit from the transformation. Lack of specificity of enzymes and cofactors, typically induced by growth substrate, permits the fortuitous degradation of non-growth substrates. Many environmentally significant compounds have been shown to be biodegradable by co-metabolism. Methanotrophic communities have demonstrated the ability to degrade many halogenated aliphatic compounds, alkanes and aromatic compounds. Other compounds capable of being co-metabolized include: polycyclic aromatic hydrocarbons, alkyl-substituted cyclic hydrocarbons, monofluorobenzoates and polychlorinated biphenyls.

Trichloroethylene (TCE) is a chlorinated aliphatic hydrocarbon. It has been widely used as an industrial solvent and degreaser. Spillage, dumping and improper storage have caused TCE to be one of the most frequently found groundwater contaminants. Aerobic co-metabolism of TCE was first noted by Wilson and Wilson (1985). Since then, a variety of microorganisms have been shown to be capable of degrading TCE by the production of oxygenase enzymes induced by various growth substrates such as methane, propane, toluene, phenol and others. This study used phenol as a growth substrate and as an oxygenase inducing compound to aerobically degrade TCE.

Typical oxygenase co-metabolism reactions for growth substrate are presented in Figure 1-1 (Chang and Alvarez-Cohen, 1995).

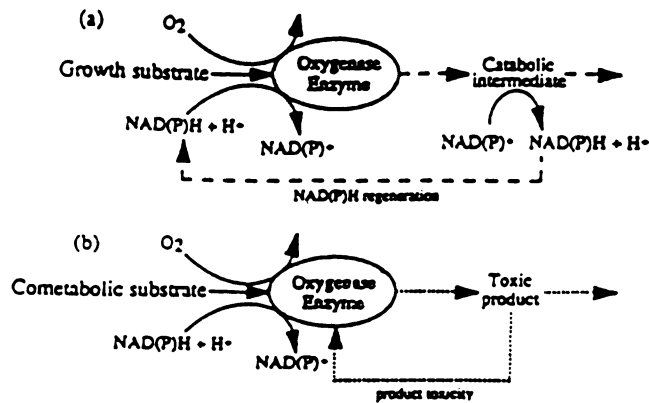


Figure 1-1 Oxygenase Mediated Co-metabolism

The above figure identifies some problems inherent in co-metabolism. First, toxic intermediates can damage the cells or the enzyme itself, reducing the cells ability to degrade non-growth substrate. Second, many co-metabolic reactions require reducing power in the form of NAD(P)H. In the absence of growth substrate to provide regeneration of NAD(P)H, it is possible that co-metabolic transformation can become limited by lack of reducing power.

Various models have been proposed to describe co-metabolism. Traditional Michaelis-Menten expressions for degradation and the Monod equation for cell growth have been shown to inadequately describe co-metabolic reactions. Alvarez-Cohen and McCarty (1991) reported that linearized Monod equations yielded artificially elevated kinetic parameter estimates. These errors result from the failure of the Michaelis-Menten/Monod equations to account for loss of transformation activity, product toxicity and competitive inhibition. Alvarez-Cohen and McCarty (1991) incorporated the effects of product toxicity by using a microbial concentration that decays in proportion to the

transformation capacity. Criddle (1993) proposed a general co-metabolism model which accounted for cell growth, endogenous decay, product toxicity, competitive inhibition, and enhancement of degradation rates by addition of growth and energy substrates. This model was evaluated experimentally and found to be satisfactory for methanotrophic co-metabolism of TCE (Chang and Criddle, 1997). Chang and Alvarez-Cohen (1995a) proposed a model that further accounted for possible loss of reducing power as a limiting factor of non-growth substrate degradation. Due to a high growth substrate to non-growth substrate ratio used in this study it was assumed that limitations due to loss of reducing power would not occur. This work proposes two models based on Criddle (1993): a one-population model in which all biomass is assumed to be capable of degrading TCE and a two-population model in which phenol degrading microorganisms are divided into two subsets - TCE degrading bacteria and non-TCE degrading bacteria.

Much of the research concerning aerobic, mixed-culture co-metabolism of TCE has been concerned with in-situ groundwater applications and chemostatic reactors, in which both growth substrate and non-growth substrate are present at the same time. However, it has been demonstrated that phenol and TCE compete for the same oxygenase enzymes.

Chang and Alvarez-Cohen (1995b) reported that although there is some apparent benefit to adding low concentrations of growth substrate (< 0.1 mM), degradation rates begin to decrease as higher concentrations (> 0.1 mM) are added. In response to these indications of competitive inhibition, intermittent feeding schemes and sequencing batch reactors have been investigated to avoid these problems (Segar et al., 1995).

Shih (1995) numerically simulated and evaluated an aerobic sequencing batch reactor that degraded TCE using phenol as a growth substrate. Using a recharge stage to feed phenol and a separate fill stage to feed TCE, competitive inhibition was avoided. Computer modeling was able to predict TCE levels in the reactor. Chang (1996) confirmed the long-term ability of a phenol-degrading community to degrade TCE. He further reported on various methods of measuring the stability of mixed microbial communities, and the effects of long-term exposure on the adaptation of communities to non-growth substrates and feeding perturbations.

In this study, a dispersed growth, aerobic sequencing batch reactor was used to co-metabolically degrade TCE using phenol as a growth substrate. Two models - a one-population model and a two-population model - are modeled by computer using kinetic parameters determined experimentally. Model predictions were compared to data gathered from the laboratory scale sequencing batch reactors. A theoretical sensitivity analysis was also performed to gauge the importance of various kinetic parameters to the model.

CHAPTER 2

MODEL DEVELOPMENT

Phenol Degradation

Cell growth is most commonly described by the Monod Equation

$$\mu = \frac{\mu_{\max} S}{K_s + S} \quad (2-1)$$

where S = substrate concentration (mg/L), μ = specific growth rate (1/day), μ_{\max} = maximum specific growth rate (1/day) and K_s is the half saturation coefficient (mg/L).

Some argument has been made that phenol is a self-inhibitory growth substrate and that it should be modeled using the Haldane expression

$$\mu = \frac{\mu_{\max} S}{K_s + S + \frac{S^2}{K_i}} \quad (2-2)$$

where K_i = inhibition constant. However, Auteinrieth et al.(1991) reported that at low phenol concentration (100 mg/L) degradation follows zero order kinetics. Shih (1995) also reported zero order degradation, with respect to substrate concentration, for a phenol concentration of 150 mg/L. In this reactor, phenol concentration remained below 30 mg/L, therefore zero order kinetics were used to model phenol degradation. Zero order kinetics are described by the equation

$$\frac{dS}{dt} = -k^0 X \quad (2-3)$$

where k^0 is the zero-order rate constant (mg phenol/mg biomass - day) and X is the biomass concentration (mg/L). This expression for substrate degradation may be combined with the following relationship:

$$Y\left(-\frac{dS}{dt}\right) = \mu X \quad (2-4)$$

where Y = yield of unit biomass per unit substrate (mg cells/mg substrate), yielding

$$\mu = Yk \quad (2-5)$$

This equation, however, represents growth only. To obtain a net specific growth rate, an endogenous decay term is added to represent cell death, cell lysis, etc.

$$\mu = Yk^0 - b \quad (2-6)$$

where b = endogenous decay rate (1/day). This equation represents the net specific growth rate expression for growth on phenol used in this study.

Change in biomass concentrations is expressed by the equation

$$\frac{dX}{dt} = \mu X \quad (2-7)$$

Where X is the concentration of active phenol-degrading biomass (mg/L). Combining equation (2-7) with (2-6) yields

$$\frac{dX}{dt} = Yk^0X - bX \quad (2-8)$$

which represents the growth of phenol-degrading cells.

Some phenol-degrading cells are known to be capable of degrading TCE by co-metabolism, while others are not. It is possible, then, to divide the population of phenol degrading cells into two sub-populations: TCE-degrading cells and non-TCE-degrading cells. This division of population, however, presents experimental difficulties in the enumeration of the subdivisions. In this study, two models were developed and tested: a two-population model, in which microorganisms are classified as described above, and a one-population model, which views the microbial population as completely comprised of TCE-degrading organisms. Model development continues along these two courses.

Two Population Model

In this model, biomass capable of degrading phenol was subdivided into fractions that can degrade TCE, X_{apt} , and that cannot degrade TCE, X_{ap} , where subscripts denote: a, active organisms, p, phenol-degrading organisms, and t, TCE-degrading organisms. These fractions, however, cannot be differentiated experimentally. It is possible, however, to indirectly measure the specific growth rate of fraction X_{apt} , μ_{apt} (Chapter 3). Thus, an expression for X_{apt} can be created:

$$\frac{dX_{apt}}{dt} = \mu_{apt} X_{apt} \quad (2-9)$$

where μ_{apt} = the specific growth rate. This method of determining this rate includes effects of endogenous decay and therefore equation 2-9 needs no further modification. However, for periods during which no TCE is present, a corresponding endogenous decay for the TCE degrading population, b_{apt} , must similarly be developed.

Determined experimentally, μ_{apt} represents the increase in ability to degrade TCE. This increase may not reflect an increase in actual cells, rather, it may only represent an increase in the ability of each cell to degrade TCE (e.g. increase in oxygenase enzyme, replenishing of reducing power). This model assumes that the increase is an actual increase in cells, as to assume otherwise would demand first the determination of what process(es) contribute to increased ability to degrade TCE and second, direct enumeration of such process(es). These ventures are beyond the scope of this study.

Total active biomass, then, is defined as

$$X_a = X_{ap} + X_{apt} \quad (2-10)$$

Expressions for the various types of biomass and phenol concentration can be created:

$$\frac{dX_a}{dt} = \frac{dX_{ap}}{dt} + \frac{dX_{apt}}{dt} \quad (2-11)$$

$$\frac{dX_{ap}}{dt} = Yk^o X_{ap} - bX_{ap} \quad (2-12)$$

$$\frac{dS}{dt} = -k^o X_a \quad (2-13)$$

It should be noted that Y , b and k^o are all assumed to be the same for each division of biomass. Equations (2-9), and (2-11) through (2-13) comprise the expressions used to model phenol concentrations and growth of biomass in this work. Other forms of biomass assuredly exist in the reactor: predators, heterotrophic microorganisms feeding on decaying cells and degradation by-products, etc. Accurate differentiation of these groups, however, was not possible and is not addressed by this study.

One Population Model

The one population model assumes that all biomass is TCE-degrading biomass.

Concerning growth on phenol and degradation of phenol, the model may be described by equation (2-8) and a simple reform of equation (2-13):

$$\frac{dX_{apt}}{dt} = Yk^o X_{apt} - bX_{apt} \quad (2-14)$$

$$\frac{dS}{dt} = -k^o X_{apt} \quad (2-15)$$

TCE Degradation

Various models have been introduced to describe co-metabolic reactions. Alvarez-Cohen and McCarty (1991) demonstrated the failure of traditional kinetics to adequately account for significant properties of co-metabolism such as the loss of ability to degrade non-growth substrate during exposure. They introduced the transformation capacity concept. Transformation capacity is defined as

$$T_c^b = \frac{dC}{dX} \quad (2-16)$$

where dC is the mass of contaminant transformed (mg) and dX is the mass of cells inactivated by the transformation (mg). This equation, is linked with traditional Michelis-Menten degradation kinetics

$$\frac{dC}{dt} = -\frac{kC}{K_s + C} X \quad (2-17)$$

and upon integration of equation 2-16, yields the following model for substrate concentration:

$$\frac{dC}{dt} = -\frac{k C(X_o - \frac{1}{T_c^b}(C_o - C))}{K_s + C} \quad (2-18)$$

where X_o = initial biomass concentration, K_s is the half saturation coefficient (mg/L) and k is the maximum substrate utilization rate (mg substrate/mg cell - day). This equation describes degradation of non-growth substrate in the absence of growth substrate for resting cells. Criddle (1993), however, commented that the above model neglects endogenous decay and thus transformation capacity studies were measurements of the observed biomass transformation capacity rather than the true biomass transformation capacity, T_c^{b*} . The true biomass transformation capacity is defined as the mass of non-growth substrate transformed by a unit mass of cells in the absence of endogenous decay. The relationship between T_c^b and T_c^{b*} is expressed:

$$T_c^b = \frac{1}{\frac{b}{q_c} + \frac{1}{T_c^{b*}}} \quad \text{where} \quad q_c = \frac{kC}{K_s + C} \quad (2-19)$$

for resting cells. The expression for q_c assumes that TCE degradation follows traditional Michaelis-Menten kinetics. Others have reported degradation kinetics that are first order with respect to TCE concentration (Dabrock et al., 1992; Henry and Grbic'-Galic' 1990; Oldenhuis et al., 1989),

$$q_c = k'C \quad (2-20)$$

This expression can be used to augment Criddle's general model for co-metabolic reactions in the absence of growth substrate:

$$\mu = -b - \frac{1}{T_c^{b*}} k' C \quad (2-21)$$

which can be rewritten to describe biomass:

$$\frac{dX_{apt}}{dt} = -bX_{apt} - \frac{X_{apt}}{T_c^{b*}} k' C \quad (2-22)$$

where the subscripts a, p and t denote active biomass, phenol degrading biomass and TCE degrading biomass, respectively. This equation, coupled with a first order expression for substrate degradation,

$$\frac{dC}{dt} = -k' CX_{apt} \quad (2-23)$$

constitute a model for the degradation of non-growth substrate in the absence of growth substrate. It should be noted that this model assumes that all cell death due to TCE degradation occurs only among the population capable of carrying out such degradation, X_{apt} .

Mass Balance Equations

The sequencing batch reactor modeled in this study has five distinct stages: fill, react, settle, decant and recharge. The recharge stage can be further divided into two stages: recharge-fill and recharge-react. Mass balance equations for these stages must be developed. Development of these equations is similar for both the two-population and one-population models. Except where noted specifically, equations may be applied to both models with the exclusion, of course, of all equations dealing with X_{ap} , which pertain only to the two-population model.

Fill Stage

During the fill stage, 1.00 liter of influent containing TCE was fed to the reactor over a time period of 60 minutes. Dilution, degradation, air stripping and sorption to biomass can affect the concentration of TCE. Sorption of TCE to biomass has been shown to be a negligible removal process (Shih, 1995) for similar reactors with similar biomass concentrations. Loss of volatile compounds to air stripping in a sequencing batch reactor can be described by the equation

$$r_{\text{strip}} = K_{L,a}(C - C^*) \quad (2-24)$$

where $K_{L,a}$ = overall mass transfer coefficient (1/hr), C = liquid concentration of contaminant (mg/L) and C^* is the liquid phase concentration at equilibrium (mg/L). In a reactor where the volume is changing, $K_{L,a}$ will change. In this study, the following empirical relationship between $K_{L,a}$ and reactor volume for TCE was determined experimentally (Appendix B)

$$K_{L,a} = 1.73892(V^{-1.28922}) \quad (2-25)$$

where V is the reactor liquid volume (L). C^* is defined

$$C^* = \frac{C_g}{H} \quad (2-26)$$

where C_g is the gaseous phase concentration (mg/L) and H is the dimensionless Henry's constant for TCE. In this study, a dimensionless Henry's constant of 0.392 was used (Gosset, 1987).

An initial mass balance equation for TCE in the reactor liquid can be written

$$\frac{d(CV)}{dt} = C_o Q - C_g Q_g - k' X_{apt} CV - K_{L,a} (C - C^*) V \quad (2-27)$$

where C_o = TCE concentration in influent (mg/L), Q = Influent flowrate (L/hr), Q_g = Air flowrate through reactor and V is the reactor liquid Volume (L). The terms in the equation represent the following: mass in influent, mass in exhaust gas, mass removed by microbial degradation and mass removed by air stripping. Separating the left side of the equation and noting that $dV/dt = Q$:

$$\frac{dC}{dt} V = C_o Q - C_g Q_g - k' X_{apt} CV - K_{L,a} (C - C^*) V - CQ \quad (2-28)$$

Dividing through by V and further manipulation yields

$$\frac{dC}{dt} = (C_o - C) \frac{Q}{V} - C_g \frac{Q_g}{V} - k' X_{apt} C - K_{L,a} (C - \frac{C_g}{H}) \quad (2-29)$$

TCE degrading biomass will undergo three processes during the fill period, dilution, endogenous decay and decay due to product toxicity. A mass balance may be written:

$$\frac{d(X_{apt} V)}{dt} = -b X_{apt} V - \frac{q_c}{T_c^{b*}} X_{apt} V \quad \text{where } q_c = k' C \quad (2-30)$$

which, upon separation, rearrangement and substitution of $dV/dt = Q$, yields

$$\frac{dX_{apt}}{dt} = -b X_{apt} - \frac{q_c}{T_c^{b*}} X_{apt} - \frac{Q}{V} X_{apt} \quad (2-31)$$

Active cells that do not degrade TCE, X_{ap} , undergo only dilution and endogenous decay

$$\frac{dX_{ap}}{dt} = -bX_{ap} - \frac{Q}{V}X_{ap} \quad (2-32)$$

Equations (2-27), (2-29) and (2-30) represent a model for the fill stage for substrate and biomass concentrations.

React Stage

The react stage is identical to the fill stage in every respect with the exception of dilution.

Batch kinetics result, and equations (2-27), (2-29) and (2-30) reduce to the following:

$$\frac{dC}{dt} = -C_g \frac{Q_g}{V} - k'X_{apt}C - K_{L,a}(C - \frac{C_g}{H}) \quad (2-33)$$

$$\frac{dX_{apt}}{dt} = -bX_{apt} - \frac{q_c}{T_c^{b*}}X_{apt} \quad \text{where } q_c = k'C \quad (2-34)$$

$$\frac{dX_{ap}}{dt} = -bX_{ap} \quad (2-35)$$

Settle Stage

During the settle stage, neither growth substrate nor non-growth substrate will be present.

Only anoxic endogenous decay will occur. To avoid complex equations dealing with sludge settling rates, equations for biomass will be based on mass rather than concentration using the entire liquid volume as a control volume. The mass balance equations for biomass may be written as follows:

$$\frac{dM_{apt}}{dt} = -bM_{apt} \quad (2-36)$$

$$\frac{dM_{ap}}{dt} = -bM_{ap} \quad (2-37)$$

where M = mass of biomass (mg). Generally, modeling of reactor concentrations during a settling period is not of much interest. Modeling of mass however is significant, as reactions in later stages will depend on an accurate biomass prediction. Modeling during the settling stage allows for a correct initial biomass concentration condition to be calculated when the reactor returns to a completely mixed state in later stages.

Decant Stage

After the settling stage, liquid is decanted from the top of the reactor. This study assumes that all biomass settles completely during the settle stage. Therefore, mass balance equations for the decant period are the same as those used during the settle period.

Recharge Stage

During the recharge stage, phenol was added as a growth-substrate. Net cell growth and phenol degradation during the recharge-react stage is modeled by equations (2-9), (2-11) and (2-13) for the two-population model, and by equations (2-14) and (2-15) for the one-population model. However, during the recharge-fill portion of the recharge stage, dilution must also be modeled.

$$\frac{dX_{ap}}{dt} = Yk^oX_{ap} - bX_{ap} - \frac{Q}{V}X_{ap} \quad (2-38)$$

$$\frac{dX_{apt}}{dt} = \mu_{apt}X_{apt} - \frac{Q}{V}X_{apt} \quad (2-39)$$

$$\frac{dS}{dt} = \frac{Q}{V}(S^{\circ} - S) - k^{\circ}X_a \quad (2-40)$$

where S° is the influent phenol concentration.

CHAPTER 3

MATERIALS AND METHODS

Reactor Design and Maintenance

Reactor Design

The sequencing batch reactors consisted of two Wheaton Mini-fermenters. Syringe pumps were used for phenol and TCE injection. Peristaltic pumps were used for influent and effluent pumping. A timer/controller was used to control all pumping and injecting apparatus. Air was supplied by two variable control aquarium pumps set at a flowrate of approximately 100 mL/min. Tygon tubing was used for all gas flows and teflon tubing was used for all liquid flows. Reactor temperature was maintained at a constant 23 °C by cycling water from a water bath through a heating/cooling element immersed in the reactor.

Reactor Schedule and Maintenance

Table 3-1 summarizes reactor activities and volume throughout the cycle.

Table 3-1 SBR Schedule and Activity

Time	Activity	Reactor Volume
0:00-1:00	Influent Pump, TCE Pump, aeration, mixing	1225 mL → 2200 mL
1:00- 4:00	Aeration, mixing	2200 mL
4:00-5:00	Settling	2200 mL
5:00-6:00	Decant Pump	2200 mL → 1200 mL
6:00-6:30	Phenol Pump, aeration, mixing	1200 mL → 1225 mL
6:30-12:00	Aeration, mixing, manual wasting	1225 mL

One-hundred mL of reactor cells were wasted once a day (every other cycle). After wasting, 100 mL of reactor media was injected back into the reactor to make up for lost volume.

Table 3-2 lists reactor conditions.

Table 3-2 Reactor Conditions

TCE Influent Concentration	5.0 mg/L
Mass TCE Added per Cycle	5.0 mg
TCE Influent Flowrate	1.0 L/hr
Air Flowrate	100 mL/min
Phenol Influent Concentration	7200 mg/L
Mass Phenol Added per Cycle	180 mg
Phenol Influent Flowrate	50 mL/hr
Reactor Temperature	23 °C

Reagents

Trichloroethylene was obtained from Aldrich Chemicals Co., Milwaukee, WI. Reactor media contained the following compounds: 2.13 g/L Na_2HPO_4 , 2.04 g/L KH_2PO_4 , 0.99 g/L $(\text{NH}_4)_2\text{SO}_4$, 66 mg/L $\text{CaCl}_2 \cdot 2\text{H}_2\text{O}$, 248 mg/L $\text{MgCl}_2 \cdot 6\text{H}_2\text{O}$, 0.5 mg/L FeSO_4 , 0.4 mg $\text{ZnSO}_4 \cdot 7\text{H}_2\text{O}$, 0.02 mg $\text{MnCl}_2 \cdot 4\text{H}_2\text{O}$, 0.05 mg/L $\text{CoCl}_2 \cdot 6\text{H}_2\text{O}$, 0.01 mg/L $\text{NiCl}_2 \cdot 6\text{H}_2\text{O}$, 0.015 mg/L H_3BO_3 and 0.25 mg/L EDTA. pH of the media was 6.8.

Initial Degradation Rate Studies

Trichloroethylene

Initial degradation rate studies of trichloroethylene were conducted by spiking sequencing batch reactor cells with trichloroethylene and measuring the decrease in trichloroethylene concentration over time. One mL of reactor liquid was added to 4 mL of reactor media in 20 mL glass vials. Three samples of each reactor were taken. The vials were then spiked with approximately 2 μ L saturated trichloroethylene solution (approximately 1100 mg/L) and crimp sealed with butyl seals. After shaking for approximately 3 minutes, 0.1 mL of headspace gas was injected into a Hewlett Packard Model 5890 gas chromatograph (GC) equipped with an electron capture detector (ECD). GC/ECD operating parameters are shown in Table 3-3. Headspace samples were injected four times at approximately 10 minute intervals.

A dimensionless Henry's constant of 0.392 for trichloroethylene (Gossett, 1987) was used to determine the liquid concentration of trichloroethylene in the vials. Using corresponding solids data, degradation rates were used to calculate k' .

Table 3-3 Gas Chromatograph Operating Parameters

<i>Parameter</i>	<i>GC/ECD</i>	<i>GC/FID</i>
Injection Temperature (°C)	250	250
Detector Temperature (°C)	350	250
Oven Temperature (°C)	90	90
Initial Temperature (°C)	90	90
Final Temperature (°C)	90	90
Carrier Flow / Gas (mL/min)	11.2 He	12.8 N ₂

Standards were prepared by injecting into the chromatograph a known volume of solution of TCE in methanol. The TCE in methanol solution was prepared by adding a weighed amount of TCE to a known volume of methanol.

Total Suspended Solids

The method used to determine the total suspended solids concentration is provided in Standard Methods (1995). Filters (0.2 μm , 47 mm diameter Gelman Sciences, Ann Arbor, Michigan) were rinsed with approximately 50 mL of deionized water, dried overnight and weighed. After filtering 5.00 mL of reactor fluid, the filters were dried overnight and weighed. The difference between the two measurements when divided by the sample volume yields the total suspended solids concentration.

Measurement of Volatile TCE Loss During Fill Cycle

TCE in the gaseous phase in the reactor was measured by injecting 0.1 mL of reactor headspace into a GC/ECD. Operating conditions of the GC/ECD are summarized in Table 3-3. Standards preparation was the same as for the initial degradation rate studies.

Measurement of Liquid Phase TCE

In order to measure liquid phase TCE concentrations during the fill and react stages, 4.93 mL samples of reactor liquid were placed into vials containing 0.07 mL of 2 N HCl solution in order to stop cell activity. Vials were crimp sealed and placed on a rotary

shaker at 300 rpm for at least 3 minutes. 0.1 mL of vial headspace was analyzed by GC/ECD.

Phenol Measurements

Phenol samples were analyzed using high pressure liquid chromatography (HPLC). Cell samples were injected into sampling vials through 0.2 μm syringe filters. The water HPLC (Perkin Elmer Series 200) was equipped with a column (Hypersil Elite C18, 4.6 mm dia., 25 cm. length, 5 μm particle size, Catalog No. 76884501) and UV detector (LC235C Photodetector) and was operated isocratically ((60% acetonitrile + 40% water) at a total flow rate of 1.0 mL/min. Detector wavelength was 255 nm and injection volume was 25 μL . Detection limit was 1 mg/L.

Phenol (obtained from J.T. Baker, purity 99.9) standards were prepared by weight.

Standards and samples were stored at 4 °C in absence of light until analysis.

Kinetic Parameters

Yield on Phenol, Y

To determine the yield on phenol, 10.0 mL of cells were removed from the reactor, placed in an Erlenmeyer flask and diluted with 90.0 mL of reactor media. The diluted cells were then injected with a known amount of phenol. The flask was shaken at 300 rpm and remained open to air to provide oxygen for aerobic metabolism. A sponge cap was used to prevent infiltration of airborne solids. At the time of cell removal, the total

suspended solids (TSS) concentration in the reactor was measured. After allowing time for phenol degradation, TSS concentration in the flask was measured. The increase in TSS was divided by the mass of phenol added to obtain Y .

It should be noted that the yield measured in this way is an “observed” yield rather than a true yield coefficient (see Chapter 4).

Specific Growth Rate of TCE-degrading Biomass, μ_{apt}

During growth on phenol, TCE degrading bacteria repair damage caused by product toxicity and are induced to produce more TCE-degrading enzyme. These phenomena cause an effective increase in the biomass capable of degrading TCE, X_{apt} . However, since direct enumeration of this fraction of the total biomass was not possible, change in biomass concentration was expressed using the specific growth rate. The specific growth rate was determined by measuring the initial TCE degradation rate for a subsample of cells, spiking those cells with phenol, and measuring the initial TCE degradation rate after the degradation of phenol was completed. Assuming that the increase in degradation rate is proportional to the specific growth rate, the specific growth rate of the TCE-degrading biomass can be effectively represented by the natural logarithm of the ratio of initial degradation rates before and after phenol consumption.

Endogenous Decay, b

Approximately 75 mL of reactor cells were removed to conduct endogenous decay experiments. The cells were placed on a shaker table in an Erlenmeyer flask capped only with a sponge to prevent airborne contaminants from entering the culture. Over a period of seven days, five biomass concentration measurements were taken. A log-normal plot of concentration vs. time yields a straight line with a slope equal to the endogenous decay rate.

Endogenous Decay of TCE Degrading Population, b_{apt}

As direct enumeration of the biomass fraction X_{apt} was not possible, the endogenous decay rate was determined indirectly, similar to the method used for the determination of μ_{apt} . Approximately 50 mL of reactor cells were removed from the reactor and placed on a 300 rpm shaker table. Periodically, sub-samples were removed and the initial degradation rate was determined. A log normal plot of the ratio of degradation rate at any time t to the rate at the beginning of the experiment versus time yields a line with slope b_{apt} .

Transformation Capacity, T_c^b

Transformation capacity experiments were conducted by spiking reactor cells with a known amount of TCE and measuring the total mass of TCE degraded. 9.75 mL of reactor cells were placed with 10.00 mL reactor media in a 45 mL screw-top amber glass vial fixed with a Mininert valve. 0.250 mL of saturated TCE solution was injected into the vial and the vial was placed on a shaker table. A reactor solids measurement at the time of cell removal provided for the calculation of mass of cells in the vial.

Measurements of TCE in the vial headspace were analyzed on a GC/FID. When TCE degradation had ended, the mass of TCE degraded was divided by the mass of cells present in the vial, yielding the observed transformation capacity.

Standards for the GC/FID were created by injecting a known amount of TCE saturated solution into a make-up volume of reactor media. The same size glass vials and Mininert valves as used in the transformation capacity determination were used for the standards preparation. The total volume of TCE solution and make-up volume was the same as that in the transformation capacity experiments.

TCE Rate Coefficient, k'

At the low concentrations observed in the reactor, TCE degradation is assumed to be first order with respect to concentration

$$\frac{dC}{dt} = k'CX_{apt} \quad (3-1)$$

Five mL of reactor cells were placed in glass vials, spiked with 4 μ L TCE saturated water and crimp sealed. TCE concentration was measured by headspace analysis using GC/ECD. A plot of the natural logarithm of TCE concentration versus time yields a straight line with a slope equal to the product of biomass concentration and k' . Dividing this determined slope by a measured biomass concentration yields the TCE rate coefficient. It should be noted that no experimental method was used to separate biomass fractions. Thus, in determining k' , a total suspended solids measurement is used rather than a true measurement of X_{apt} .

Zero-order Phenol Degradation Coefficient, k^0

Approximately 20 mL of reactor cells were removed from the reactor to determine k^0 .

The cells were spiked with phenol and subsamples were removed and filtered with syringe filters. Filtrate was analyzed for phenol concentration using high pressure liquid chromatography (HPLC). A plot of phenol concentration versus time yields a straight line with a slope equal to the product of k^0 and X_a . Dividing this slope by a biomass concentration measurement yields the zero-order coefficient, k^0 . It should be noted that the measurements used in this study to represent biomass concentrations were total suspended solids measurements, as enumeration of the different fractions of biomass was not possible.

CHAPTER 4

PARAMETER DETERMINATION

Yield on Phenol, Y

To determine yield on phenol, 10 mL of cells were removed from the reactor, placed in an Erlenmeyer flask and diluted with 90 mL of reactor media. The diluted cells were then injected with a known amount of phenol. The flask was placed on a rotary shaker table at 300 rpm and remained open to air to provide oxygen for aerobic metabolism. A sponge cap was used to prevent infiltration of airborne solids. At the time of cell removal, the total suspended solids (TSS) concentration in the reactor was measured. After allowing time for phenol degradation, TSS concentration in the flask was measured. The increase in biomass was divided by the mass of phenol added to obtain Y. Results are presented in Table 4-1.

Table 4-1 Kinetic Parameters Used in Computer Modeling

Parameter	Control	Exposed
Y (mg TSS/mg Phenol)	0.9	1.3 (1.0-1.3)
μ_{apt} (1/day)	21.5	2.7
b (1/day)	0.06-0.3	0.05 (0.02-0.3)
b_{apt} (1/day)	0.2-3.9	0.85 (0.4 - 1.3)
T_c^b (mg TCE /mg TSS)	0.38	0.29
k' (L/mg TSS-day)	-	0.2
k^o (1/day)	-	2.6 ± 1.1

*values in parentheses represent the experimental range of values

A typical yield coefficient for activated sludge is 0.6 mg/mg (Metcalf and Eddy, 1991).

Values for mixed cultures using phenol as a growth substrate range from 0.45 mg/mg (Beltrame et al., 1980) to 0.9 mg/mg (Autenrieth et al. 1991) with most reporting near 0.55 mg/mg (Kotturi et al., 1991; Chang and Alvarez-Cohen, 1995b).

It should be noted that in this study, total suspended solids was used to represent biomass. Under controlled conditions, when the influent flow is known to contain no suspended solids, this assumption is valid. Other problems, however, arise from using a TSS measurement to represent biomass in the determination of other kinetic parameters, particularly in regard to the two-population model. Kinetic parameters such as μ_{apt} and b_{apt} are theoretically specific to the sub-population X_{apt} . However, due to the inability to differentiate or separate biomass fractions, determination of these parameters had to be made using TSS measurements. This undoubtedly skewed these parameters, and perhaps contributed to the failure of the two population model (Chapter 5).

It should also be noted that this method of determining the yield coefficient produces an observed yield rather than a true yield. This method fails to discount the effects of endogenous decay during the growth on phenol. For this reason, the models do not include an endogenous decay term during those periods in the reactor when phenol concentration is greater than zero.

Observed Specific Growth Rate of TCE-degrading Biomass, μ_{apt}

During growth on phenol, TCE-degrading bacteria repair damage caused by product toxicity and are induced to produce more TCE-degrading enzymes. These phenomena cause an effective increase in the biomass capable of degrading TCE, X_{at} . Typical representations of changes in biomass, such as the yield coefficient, however, could not

be determined directly due to the inability to differentiate between fractions of biomass (i.e. active biomass, inactive biomass, TCE-degrading biomass, non-TCE degrading biomass, etc.). Consequently, an indirect expression of biomass change was required.

An assumption was made that the ability to degrade TCE is proportional to the concentration of TCE-degrading biomass. Based on that assumption, a semi-log plot of the ratio of initial TCE degradation rates before and after phenol consumption versus time will yield a straight line with a slope which effectively represents the specific rate of growth of TCE-degrading biomass. Expressed mathematically,

$$\mu_{apt} = \frac{\ln\left(\frac{dC}{dt}\right)_t - \ln\left(\frac{dC}{dt}\right)_o}{t_t - t_o} \quad (4-1)$$

where dC/dt represents the initial degradation rates (mg/L/hr), t is time (hours) and subscripts t and o represent the time after phenol consumption and before phenol addition, respectively. Results of μ_{apt} experiments are presented in Table 4-1.

Almost an order of magnitude difference exists between the control reactor and the exposed reactor measurements of μ_{apt} . It is possible that the TCE-degrading population in the exposed reactor must devote more energy and mass to repairing damage done to the cells during TCE exposure, which the control reactor does not undergo. This lack of damage may also permit the phenol-induced control reactor cells to more quickly create oxygenase enzymes, thus increasing their ability to degrade TCE.

Endogenous Decay Coefficient, b

The aerobic decay coefficient for all biomass was determined by placing approximately 75 mL of reactor cells on a shaker table in an Erlenmeyer flask capped with a sponge to prevent airborne contaminants from entering the culture while maintaining aerobic conditions. Over a period of seven days, five biomass concentration measurements were made. A log-normal plot of concentration versus time yielded a straight line with a slope equal to the endogenous decay rate, b .

A large range of values for b were observed. The reason for this is unknown. Experiments were conducted during the same period of the SBR cycle. Observation of other parameters such as solids concentration and phenol degradation rates have shown variability in the reactors over time. It is possible that endogenous decay rates vary as well, however there is not enough long-term data to support any conclusion.

TCE-degrading Biomass Decay Coefficient, b_{apt}

As with the specific growth rate, the determination of b_{at} was limited by the inability to directly enumerate the population of TCE-degrading microorganisms. Consequently, a similar indirect method of measurement was employed. An aerated flask containing approximately 50 mL of reactor cells was capped with a sponge and placed on a shaker table at 300 rpm. Periodically, cells were removed to determine the initial rate of TCE degradation. This rate is used as an indication of the remaining active TCE-degrading population. A semi-log plot of the ratio of the degradation rate at any time to the

degradation rate at the start of the experiment was plotted versus time. The slope of this plot was equal to the decay coefficient, b_{at} .

Transformation Capacity, T_c^b

Transformation capacity experiments were conducted by spiking reactor cells with a known amount of TCE and measuring the total mass of TCE degraded. 9.75 mL of reactor cells were placed with 10.00 mL reactor media in a 45 mL screw-top amber glass vial fixed with a Mininert valve. 0.250 mL of saturated TCE solution was injected into the vial and the vial was placed on a shaker table. A reactor solids measurement at the time of cell removal provided for the calculation of mass of cells in the vial.

Measurements of TCE in the vial headspace were analyzed on a GC/FID. When TCE degradation ceased, the mass of TCE degraded is divided by the mass of cells present in the vial, yielding the observed transformation capacity.

Zero-Order Phenol Degradation Coefficient, k^o

k^o was determined by spiking a known concentration of reactor cells with phenol and observing phenol concentrations over time. Three flasks containing the same amount of reactor liquid were spiked with varying amounts of phenol. Sub-samples from the flasks were removed periodically and filtered to stop phenol degradation. The subsamples were then analyzed by HPLC and the data was plotted versus time, yielding a straight line with a slope, when divided by biomass concentration, equal to the zero-order degradation coefficient.

TCE First-Order Rate Coefficient, k'

Five mL of reactor cells were placed in glass vials, spiked with 4 μ L TCE saturated water and crimp sealed. TCE concentration was measured by GC/ECD. A plot of the natural logarithm of TCE concentration versus time yields a straight line with a slope equal to the product of biomass concentration and k' . Dividing this determined slope by a measured biomass concentration yields the TCE rate coefficient. It should be noted that no experimental method was used to separate biomass fractions. Thus, in determining k' , a total suspended solids measurement is used rather than a true measurement of X_{apt} .

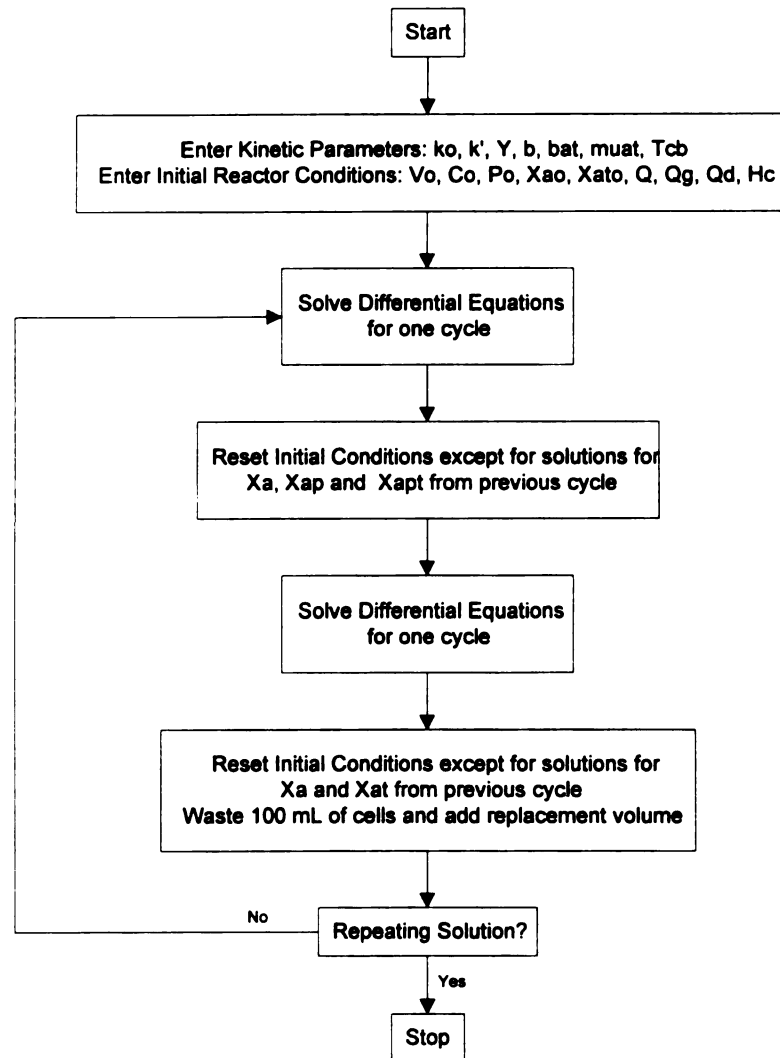
CHAPTER 5

COMPUTER MODELING AND EXPERIMENTAL VERIFICATION

MathCAD Modeling

Mathematical expressions developed in Chapter 2 to describe the sequencing batch reactor system were modeled using MathCAD software. The MathCAD software uses a fourth order Runge-Kutta approximation method to solve differential equations. A flowchart of the MathCAD programming logic is presented in Figure 5-1. Appendix A contains MathCAD worksheets and an explanation of the programming language used in the two-population model.

Figure 5-1 MathCAD Programming Logic



Experimental Results

TCE During Fill and React Stages

Liquid and gaseous phase TCE concentrations were measured during the fill and react stages on two separate occasions (Figure 5-2).

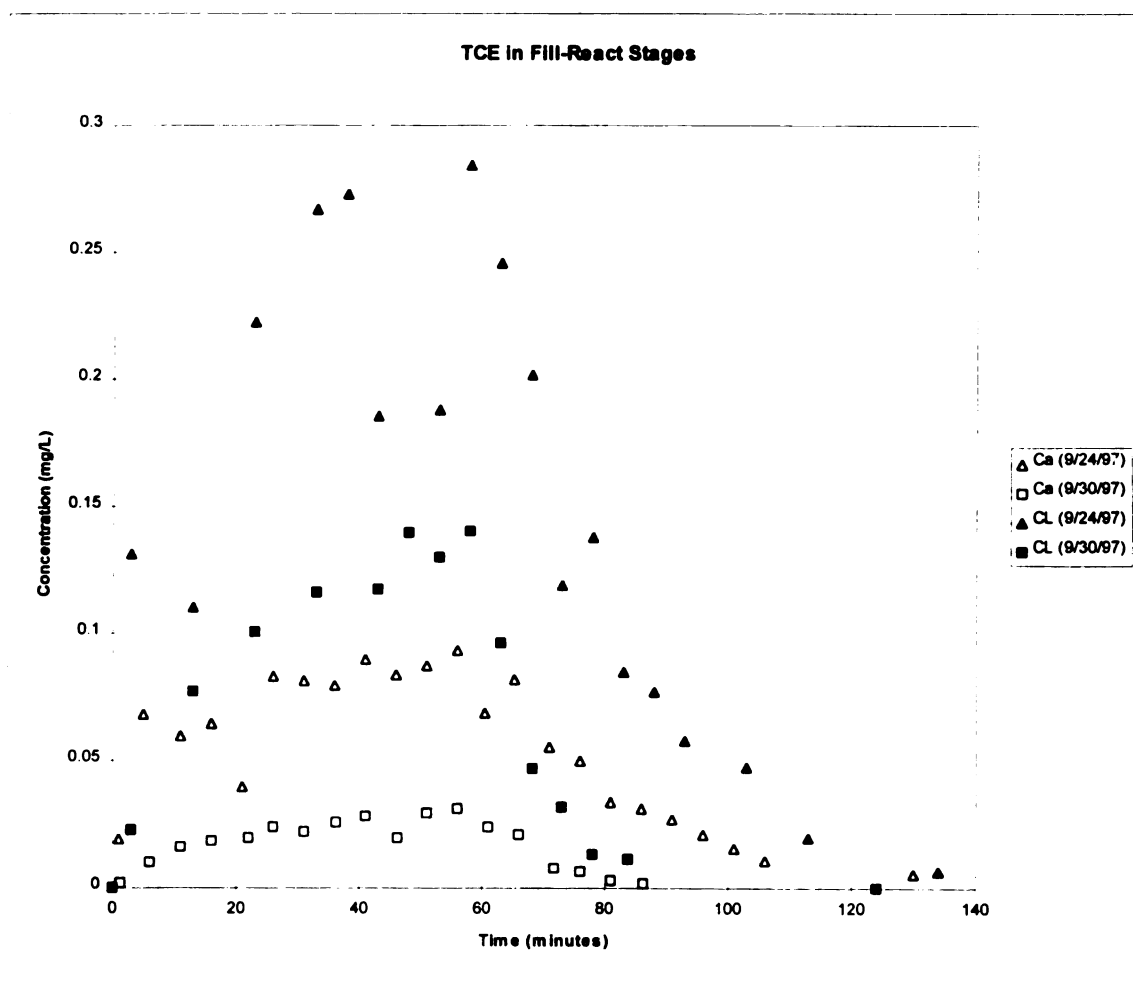


Figure 5-2 TCE in the Reactor

From these measured values, it is possible to estimate the mass of TCE lost to air stripping. The rate of mass lost to air stripping is described by the equation

$$\frac{dM_{\text{airstrip}}}{dt} = Q_g C_g \quad (5-1)$$

where Q_g is the airflow rate through the reactor (L/hr) and C_g is the gaseous concentration in the reactor headspace (mg/L). If airflow is constant, then total mass lost to air stripping may be described by the equation

$$M_{\text{airstrip}} = Q_g \int_0^t C_g dt \quad (5-2)$$

In this case, the integral was approximated using the trapezoidal rule. TCE loss for the two sampling events was 0.64 mg and 0.16 mg for 9/24/97 and 9/30/97, respectively.

These losses due to air stripping account for 12.8 % and 3.1 % of TCE introduced during the fill cycle.

Phenol During Recharge Stage

Phenol was measured in the reactor on two separate occasions, 10/6/97 and 10/24/97.

Data is presented in Figure 5-3. Due to slight variations in the speed of the syringe pump which provides phenol to the reactor, the end of phenol injections does not occur exactly at 30 minutes. Therefore, decline in phenol values sometimes began before 30 minutes.

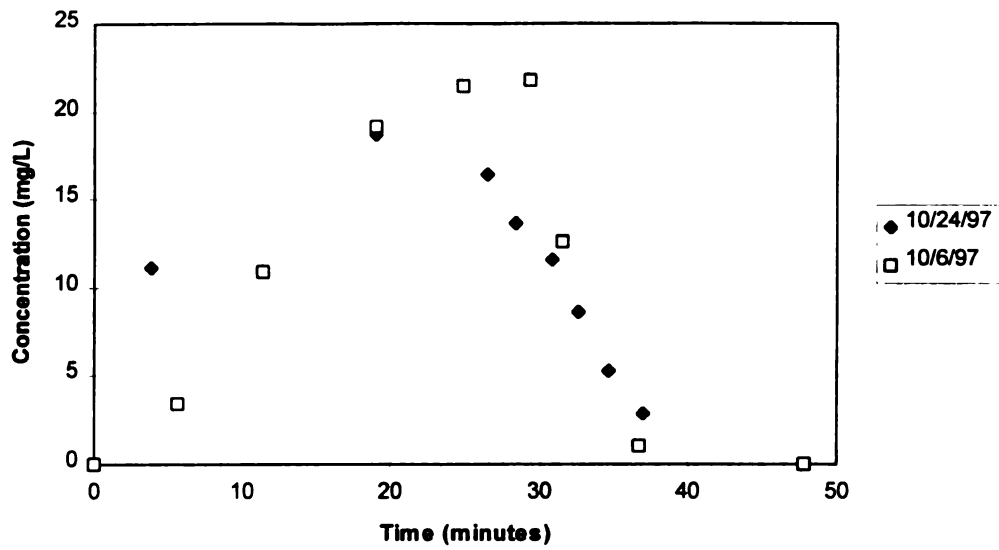
Phenol During Recharge

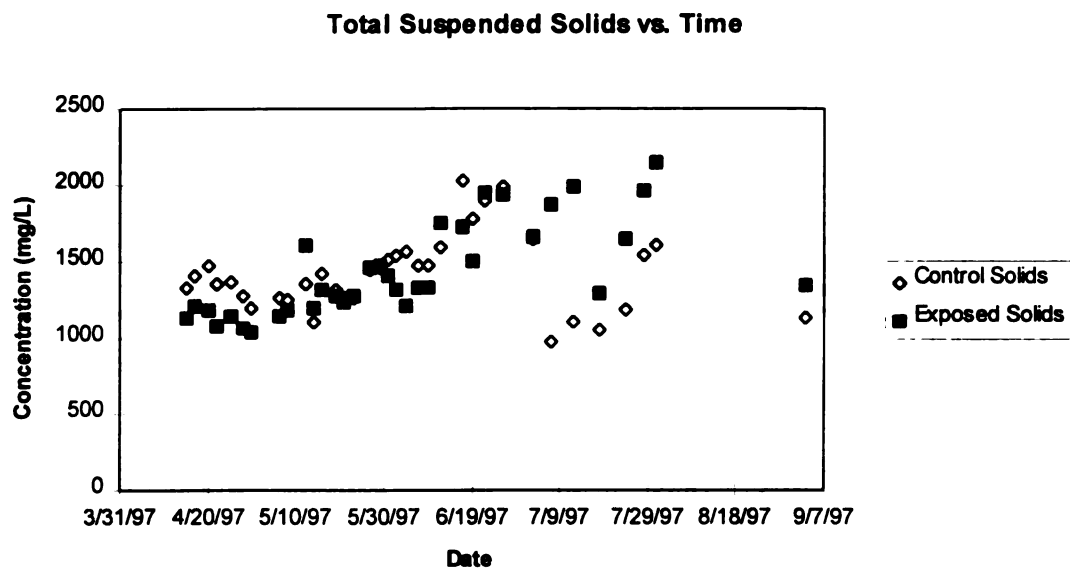
Figure 5-3 Phenol in the Reactor

Total Suspended Solids

Total suspended solids measurements were taken over a long period of reactor operation.

These measurements were used in calculations to represent active biomass, X_a , as differentiation of biomass fractions was not possible. Data is presented in Figure 5-4.

Figure 5-4 Solids Concentration over Time



One Population Model

Using the parameters contained in Table 4-1, the one population model predicts repeating solutions for biomass concentration, gaseous phase TCE concentration, liquid phase concentration, phenol concentration and cumulative mass lost to air stripping (Figure 5-5).

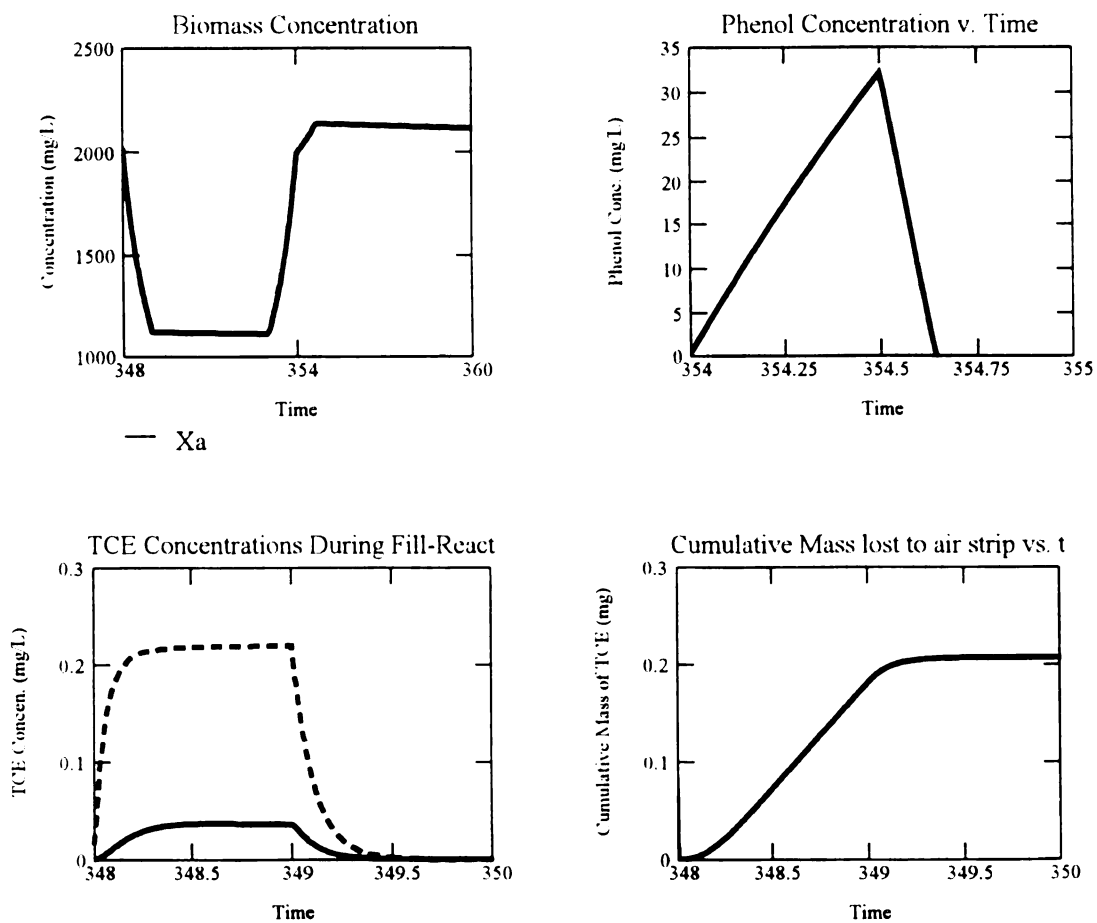


Figure 5-5 One-population Model Predictions
 $k' = 0.2$ L/mg-day, $k^o = 2.6$ 1/day, $T_{cb} = 0.29$ mg/mg,
 $Y = 1.3$ mg/mg, $b = 0.05$ 1/day

Discussion

The model predicts a repeating solution biomass concentration of approximately 2100 mg/L during the recharge stage. The measured solids concentration data is presented in Table 5-1.

Table 5-1 Solids Data

Reactor	Average Concentration (mg/L)	Standard Deviation (mg/L)	High (mg/L)	Low (mg/L)	Median (mg/L)
Control	1418	249	2030	970	1410
Exposed	1440	307	2140	1040	1330

Comparing the model with the data, it can be seen that the model overestimated the biomass concentration. This is possibly due to the failure of the model to account for predator-prey interactions known to take place in the reactor (microscopic observation verified the presence of multi-cellular organisms such as rotifers).

Figure 5-6 contains a plot of the model predictions and measured data for TCE in the reactor. The model predicted the liquid TCE concentration to reach a maximum level of 0.22 mg/L and the measured maximum values were 0.27 mg/L and 0.14 mg/L. The duration of degradation, however was not as well predicted. The model requires 90 minutes to degrade the TCE, whereas the measured values showed TCE present in the reactor as long as 140 minutes.

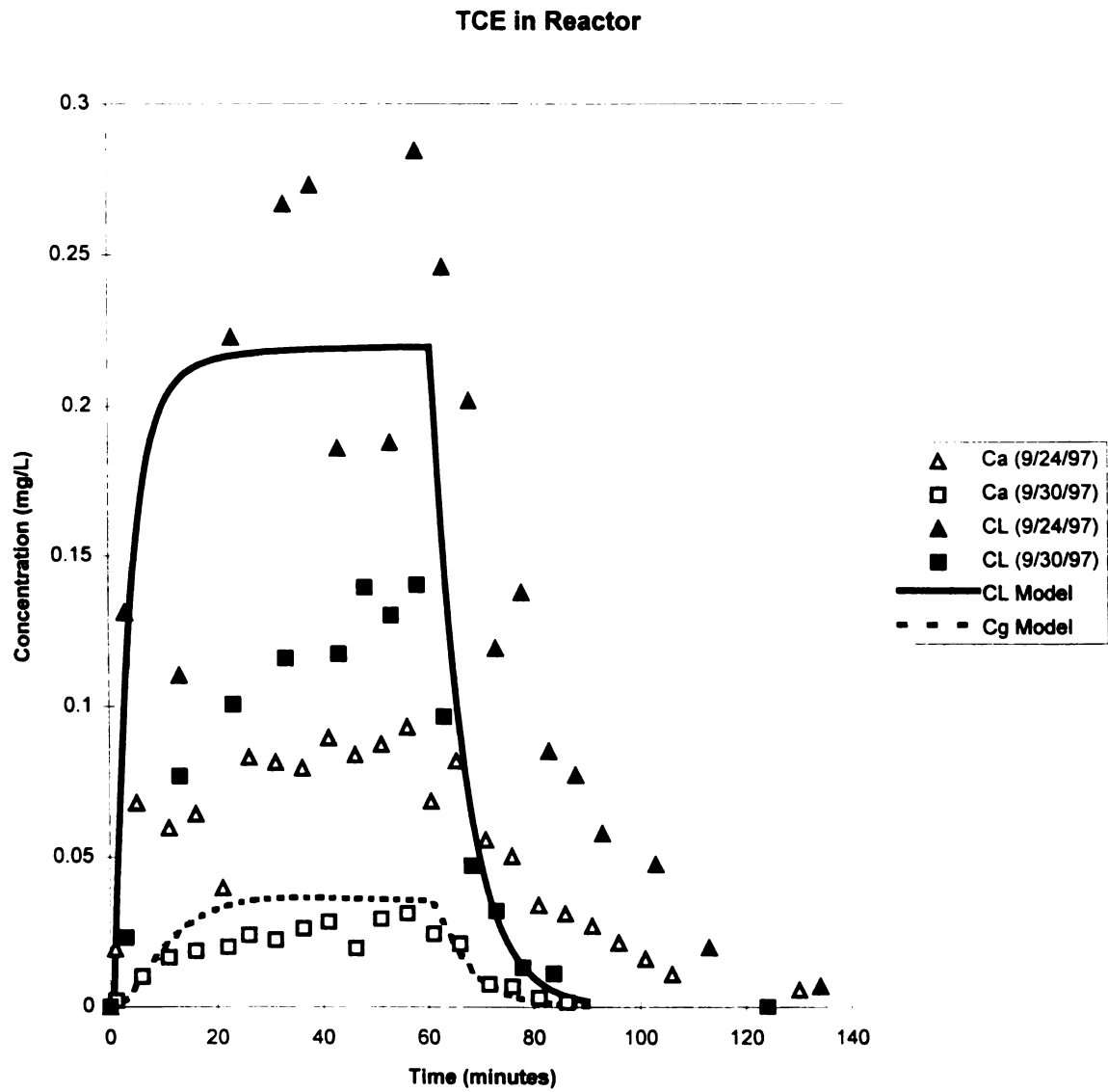


Figure 5-6 TCE Model and Data

This difference presents an interesting problem. Experimentation with the model showed that if the first order rate coefficient for TCE, k' , is decreased in an attempt to lengthen the time of TCE degradation, the peak concentration also increases. It is most likely then, that a combination of changes in parameters is required. For example, a decrease in the k' value, coupled with an increase in the mass transfer coefficient, would result in the desired lengthening of degradation time while the increased influence of air stripping would decrease the peak liquid concentration.

It should be noted that the method used to determine the liquid TCE concentration provides more opportunity for error than the method used to determine gaseous TCE concentration. This inherent error in the method may necessitate manipulation of the data to give an improved sense of where the data may actually lie. A running-average analysis of the data, for example, may yield data that more closely resembles the prediction of the model.

Further, the uncertainty analyses performed over the range of parameter values (Chapter 6) indicate that with a change in kinetic parameters, large changes in model predictions may result. Considering the variability of the experimental system as evidenced by observed changes over time in some kinetic parameters, model predictions would also fluctuate over a range large enough to encompass both data sets.

Gaseous TCE modeling was more successful. The concentration was predicted to reach 0.04 mg/L and the measured peaks were 0.03 mg/L and 0.09 mg/L. The model predicted the disappearance of TCE in the reactor headspace very well, particularly with the data set from 9/30/97. The model predicts a ratio of peak gaseous concentration to peak liquid concentration of 0.166 whereas the measured ratios were 0.32 and 0.22. This difference between the model and actual measurements may indicate that the mass transfer of TCE between the two phases is not adequately described by the $K_{L,a}$ relationship observed experimentally (Appendix B).

The mass lost to air stripping was predicted to be 0.215 mg or 4.3% of the mass injected. Estimates based on the measured gaseous TCE concentrations in the reactor were 0.64 mg (12.8%) and 0.16 mg (3.2%) for 9/24/97 and 9/30/97, respectively. The large range in measurements reflects the variability of the experimental system as a whole. This variability was also evident in other parameters.

Figure 5-7 presents phenol data along with the one-population model prediction. The model overestimates the peak concentration however the slope of the post-fill degradation curve (> 30 minutes) is similar to the data sets. More disturbing than the model's overestimation of peak concentration is the difference in shape between model and data. The data, while it supports a zero order rate assumption in its linear, post-fill stage, appears to follow a curve similar to a first-order reaction during the fill portion. More data however, would be needed to verify such a phenomena.

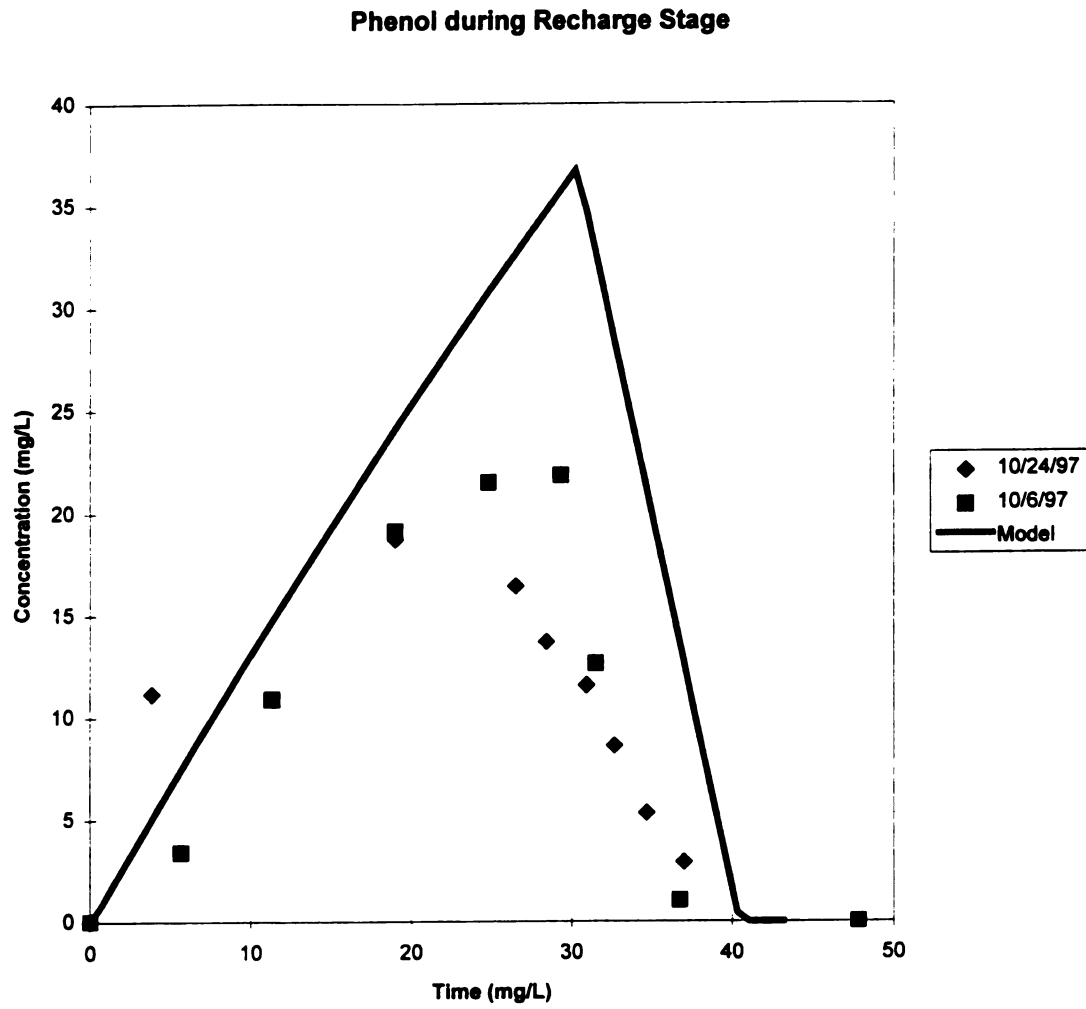


Figure 5-7 Phenol Model and Data

Two Population Model

Using the parameters experimentally determined (Table 4-1), the two-population model predicts that the phenol-degrading population, X_{ap} , becomes dominant, while the TCE-degrading biomass, X_{apt} , declines to zero. After experimenting with various changes to kinetic parameters, it was found that in every case either X_{apt} or X_{ap} became dominant, with the other population declining to zero. This phenomena indicates a problem inherent with modeling any two populations which consume the same growth substrate: differences in net growth rate will, in time, demand that one population becomes dominant. The fact that multi-population cultures exist indicate a problem with this two-population model. This model contains no limiting factor that can restrain a population from becoming dominant. A predator-prey relationship may be one method of applying such a limit.

Certainly other modeling techniques for such a system should be explored. Possible alternatives include modeling TCE-degrading microorganisms as a subset, rather than separate, of the phenol-degrading population, modeling TCE-degrading capability as a function of oxygenase enzyme level within the greater phenol-degrading population and modeling population subsets as occupying individual “niches”, in which different organisms’ kinetics become dominant at different substrate concentrations. These techniques would avoid the competition for growth substrate problem of the model in this study.

CHAPTER 6

MODEL SENSITIVITY AND PARAMETER UNCERTAINTY

Relative Sensitivity

SBR modeling presents unique problems with sensitivity assessments. Since differential equations governing solids and contaminant concentrations vary over the cycle, and since steady-state is never truly reached, standard sensitivity analyses are not feasible. For this reason, the sensitivity of the model to each parameter was based on actual model predictions over a small range ($\pm 10\%$) of each parameter. Model differences were expressed by the relative sensitivity, defined as

$$S_{pm,ps} = \frac{\delta pm / pm}{\delta ps / ps} \quad (6-1)$$

where S is the relative sensitivity, pm = the parameter modeled for and ps is the parameter changed by $\pm 10\%$. For example, a 10% increase in the endogenous decay coefficient yields a 100 mg/L decrease in the biomass concentration which was originally 1500 mg/L. The corresponding relative sensitivity, $S_{x_{a,b}}$, would be

$$\frac{-100 \text{ mg} / \text{L} / 1500 \text{ mg} / \text{L}}{0.10} = -0.67$$

The normalization of δpm and δps by pm and ps allow a comparison to be made between sensitivity coefficients of different parameters and predictions. Values chosen for to represent pm were the maximum levels of each prediction made by the model for the cycle that was determined to be the quasi-steady-state solution.

Model Sensitivity to Parameters: Results and Discussion

Sensitivity for each modeling parameter (Y , b , T_c^b , k° , k') was assessed for each of four modeling predictions (X_{apt} , C_L , C_g , S , $M_{airstrip}$). In order to avoid sign confusion, the absolute values of the relative sensitivities for +10% and -10% of a parameter were averaged and presented in Table 6-1.

Table 6-1 Relative Sensitivity

pm → ps ↓	X_{apt}	C_L	C_g	S	$M_{airstrip}$
Y	0.98	0.90	0.89	5.42	0.93
b	0.24	0.23	0.23	0.90	0.23
T_c^b	0.13	0.13	0.13	0.50	0.13
k°	0.007	0.006	0.006	3.57	0.005
k'	0.13	0.81	0.80	0.47	0.84

The table provides powerful insight into the model. Investigation by row provides an overall sense of the importance of each parameter to the entire model. By column, the table can be used to gauge the relative importance of each parameter to a specific model output. It is apparent that the yield coefficient is the parameter that the overall model is most sensitive to whereas the zero order phenol degradation rate, k° , is the parameter least

important to the model predictions (with the exception of phenol concentration, S , of course). This would seem to indicate that biomass concentration is very important to the model, which is not surprising, as a term involving biomass is present in virtually every differential equation used to describe the system. It is perhaps this dominance that is reflected in the near constant sensitivity in four of the five rows. That is, a change in a parameter affects biomass a certain way, and since biomass is so important to the system, the sensitivity to an individual parameter is the same for nearly all model predictions.

Some other interesting trends are readily apparent in the data. For all parameters but one, k' , it appears that one predicted value, S , is most affected by a change in the parameters. Degradation of phenol is dependent solely on the zero order rate coefficient, k^0 and biomass concentration, X_{apt} . As the k^0 value is kept constant in these sensitivity analyses, this is more evidence that the biomass concentration is the most influential factor in the model. This importance demands a closer look at biomass.

Investigating column X_{apt} , it is apparent that biomass is most sensitive to the yield coefficient, followed by the endogenous decay term. T_c^b and k' , being indirectly related to X_{apt} , have near the same, low bearing on X_{apt} and k^0 has virtually no influence on biomass concentration. The yield coefficient, then, is perhaps the most important parameter to the model. This is important, since future studies should pay closer attention to a solid determination of the yield coefficient.

Similar investigations by column were conducted on the other model predictions. In all cases, the yield coefficient is the most important parameter. Beyond that, columns differed but their trends were the same: after yield, the parameters most influential on a prediction were those that were directly related to the prediction (e.g. k' for C_L , C_g and M_{airstrip} , k° for P). This dominance of the yield coefficient over even those parameters that are directly related to predictions (i.e. in the actual differential equations) further solidifies its importance.

Parameter Uncertainty

In a system that experiences fluctuations in kinetic parameters, it is essential to determine how the model predictions vary over the range of experimentally determined values for each parameter. To this end, modeling was performed over the range of determined parameter values. For those parameters with a large enough data pool (k' and k°) modeling was performed over the range bounded by the calculated standard deviation. For those parameters with only a few data (Y and b), analyses were conducted over the actual range of values, with an average value for reference. Figures 6-1 through 6-4 present modeling predictions over the range of each parameter.

Discussion

Model predictions over the range of values for the yield coefficient are presented in Figure 6-1. Biomass was particularly affected, with maximum concentration predictions ranging from approximately 2100 mg/L to 1600 mg/L. Effects on TCE degradation, mass lost to air stripping and phenol degradation were similarly affected, indicating the

importance of the yield coefficient to all aspects of the model. Application of the model to engineered systems would require a well-defined, reliable range of yield measurements.

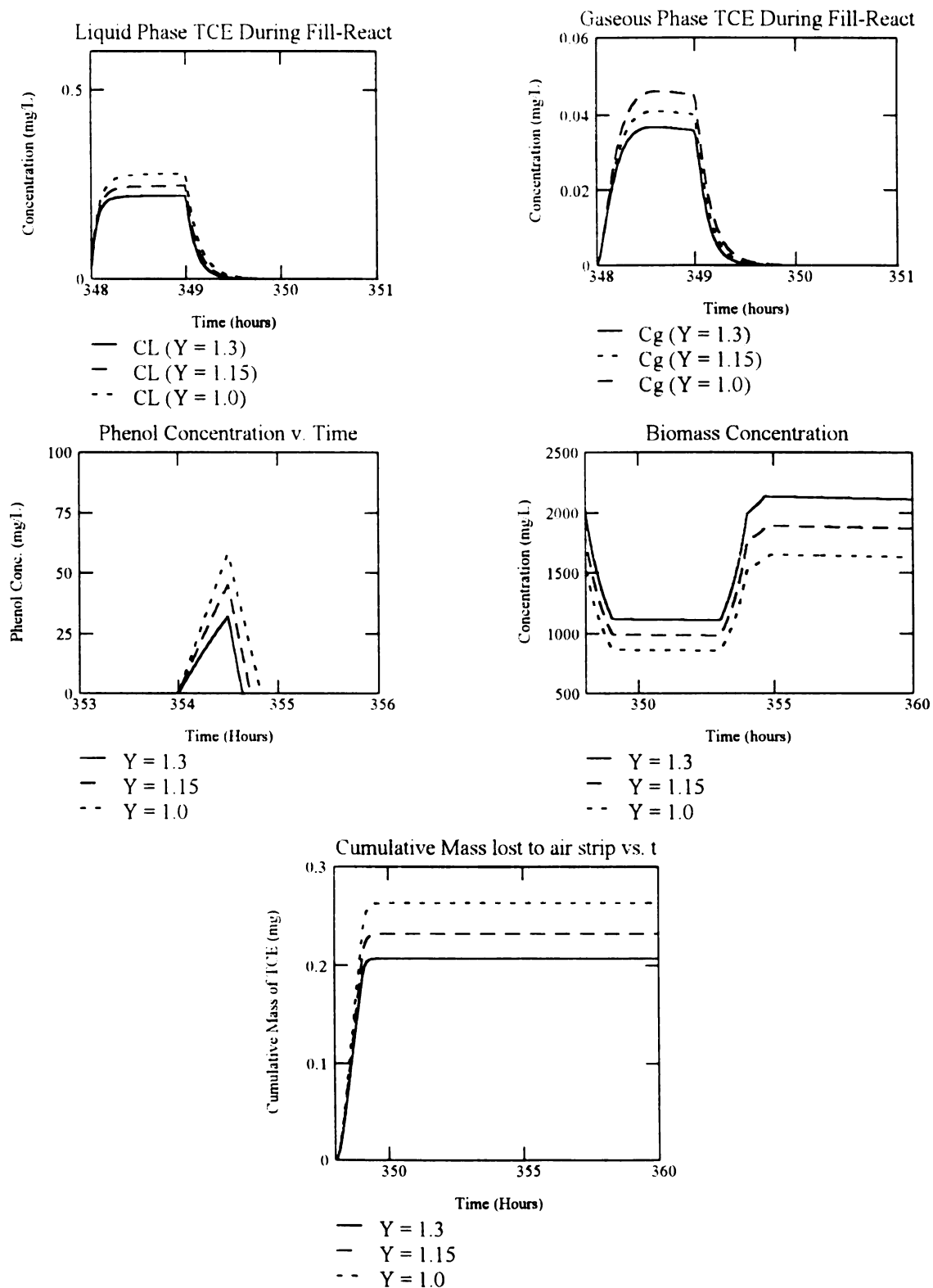


Figure 6-1 Uncertainty Modeling for Yield
 $Y = \text{variable (mg/mg)}$, $k' = 0.2 \text{ L/mg-day}$, $k^o = 2.6 \text{ 1/day}$
 $T_c^b = 0.29 \text{ mg/mg}$, $b = 0.05 \text{ 1/day}$

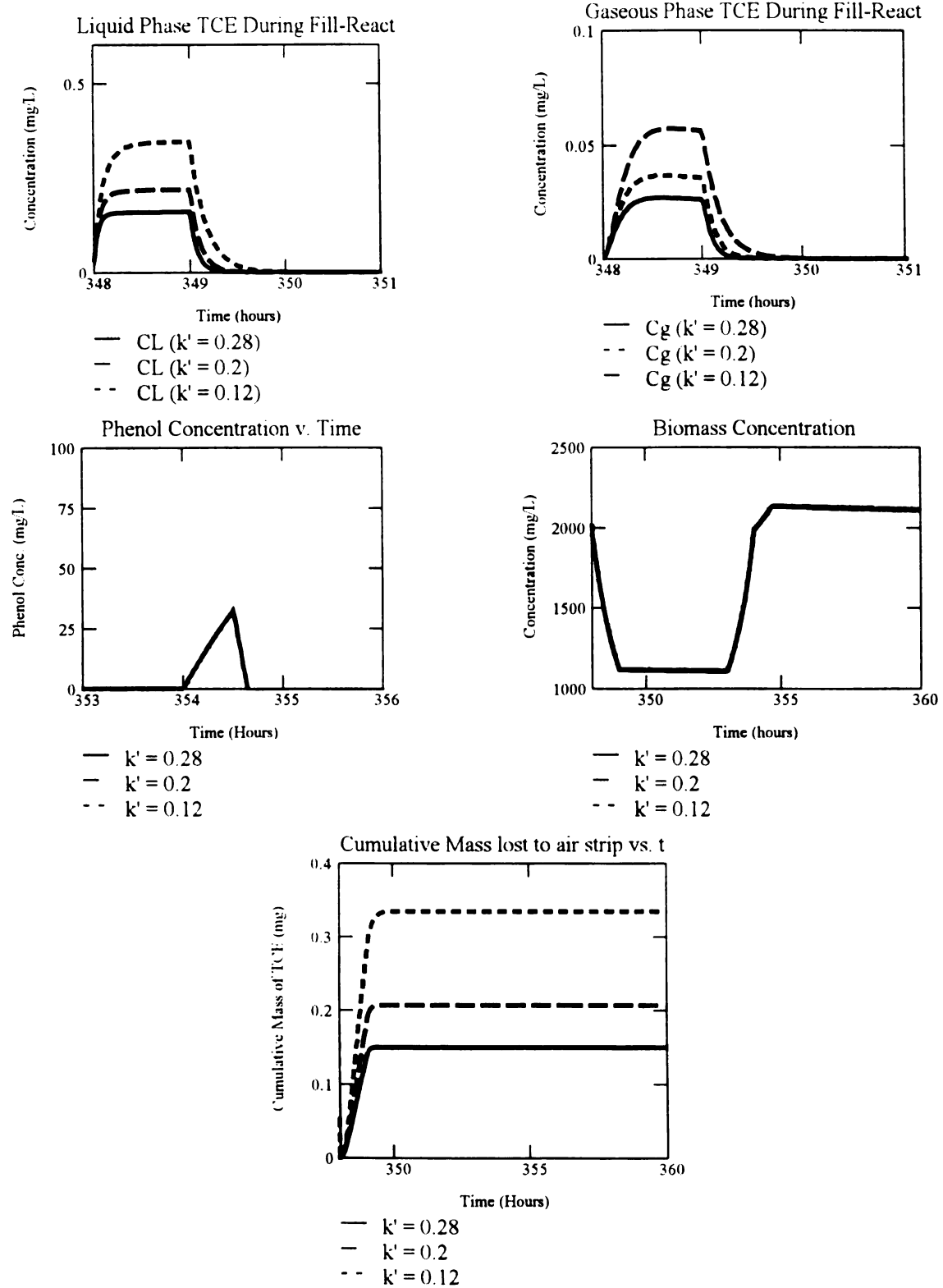


Figure 6-2 Uncertainty Modeling for k'
 $Y = 1.3 \text{ mg/mg}$, $k' = \text{variable (L/mg-day)}$, $k^o = 2.6 \text{ 1/day}$
 $T_c^b = 0.29 \text{ mg/mg}$, $b = 0.05 \text{ 1/day}$

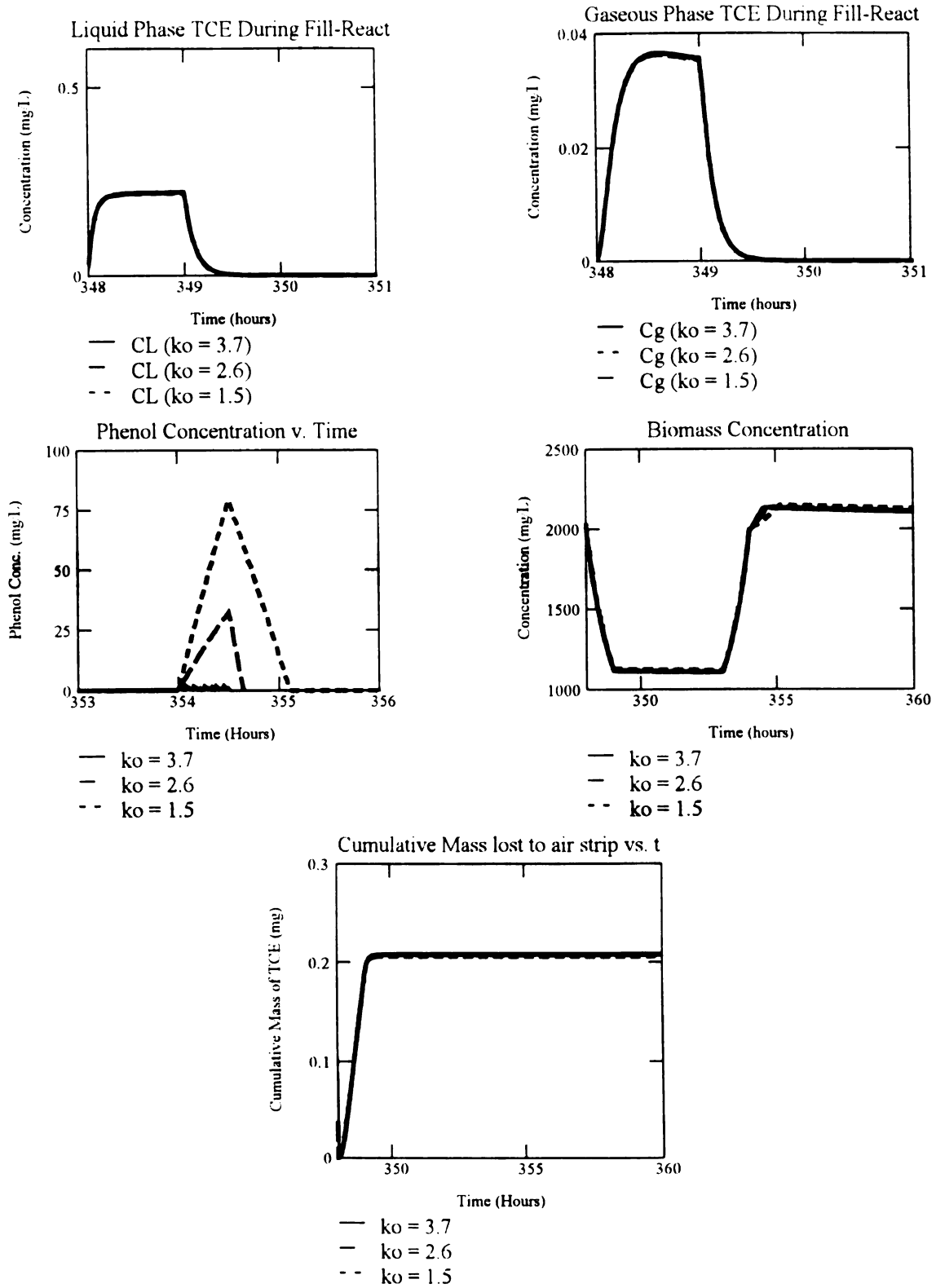


Figure 6-3 Uncertainty Modeling for k°
 $Y = 1.3 \text{ mg/mg}$, $k' = 0.2 \text{ L/mg-day}$, $k^\circ = \text{variable (1/day)}$
 $T_c^b = 0.29 \text{ mg/mg}$, $b = 0.05 \text{ 1/day}$

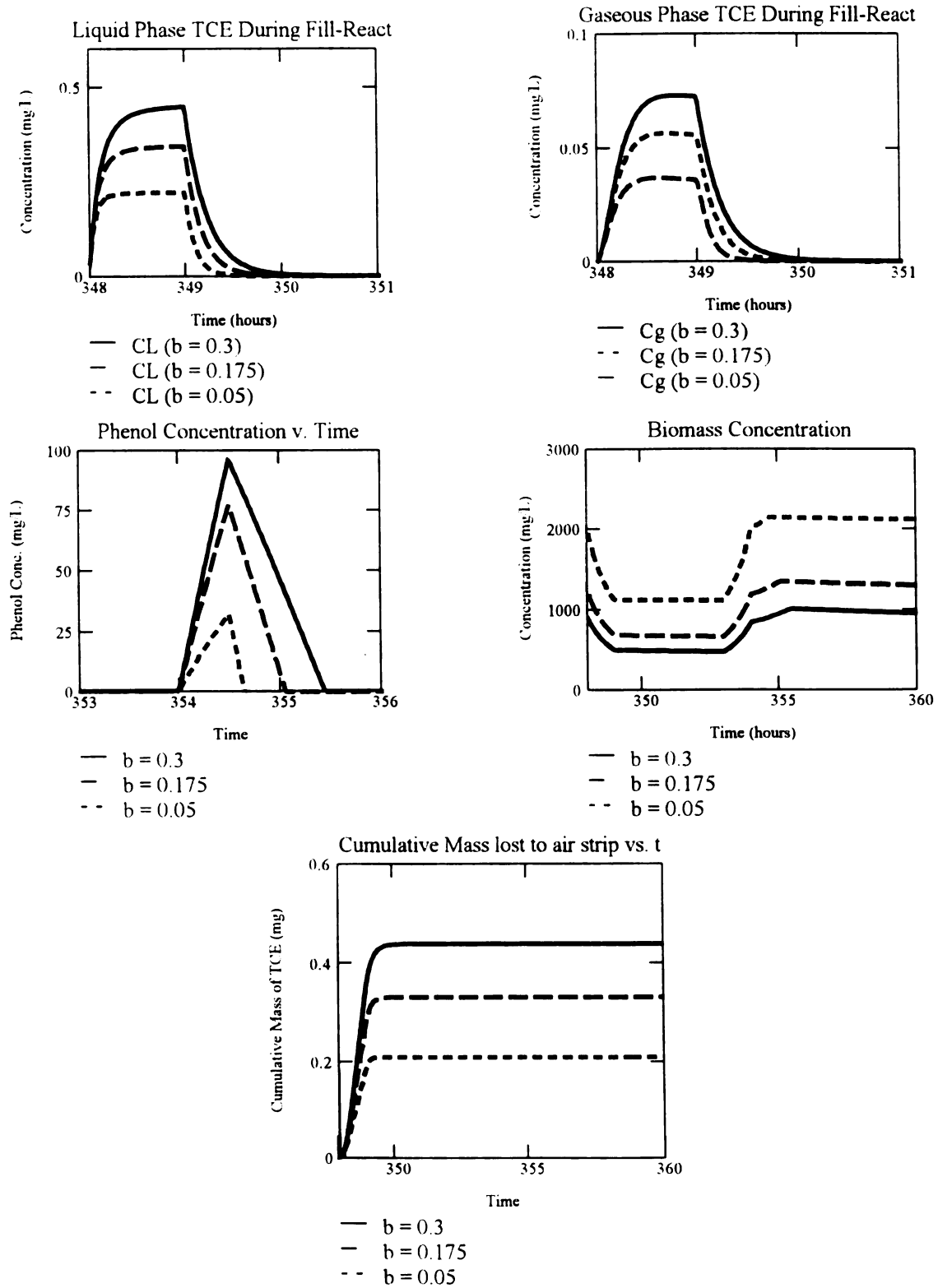


Figure 6-4 Uncertainty Modeling for b
 $Y = 1.3 \text{ mg/mg}$, $k' = 0.2 \text{ L/mg-day}$, $k^o = 2.6 \text{ 1/day}$
 $T_c^b = 0.29 \text{ mg/mg}$, $b = \text{variable (1/day)}$

Predictions over the range of k' values and k^0 values validate the conclusions drawn from the sensitivity analyses. Predictions that are not directly related to the parameter in question are not affected by changes. For k' , phenol degradation and biomass concentration are essentially unchanged. The zero-order rate coefficient for phenol degradation, k^0 has little effect on any prediction except phenol concentration. Worthy of note is the prediction for a k^0 value of 3.7 1/day, which predicted phenol to be degraded so rapidly that it produced a “sawtooth” shaped graph, an artifact that the model produces when the concentration of phenol drops below zero during the recharge-fill stage.

The large differences in the predictions based on the range of b values arise from the size of the range itself - from 0.05 to 0.3 1/day. As with the yield coefficient, b is directly related to biomass concentrations, which has a direct influence on all model predictions. This large variation in an influential parameter may be a factor in the differences between the observed data of TCE in the reactor. Here again, a larger data pool is needed to provide more reliable predictions for the model and a more satisfactory understanding of the true variability of the endogenous decay coefficient in the system.

CHAPTER 7

CONCLUSIONS AND RECOMMENDATIONS

Computer Modeling

The one-population model developed in this study adequately described TCE concentrations, both liquid and gaseous, in the reactor. Mass lost to air stripping was also within the observed range. Phenol predictions were less accurate than those for TCE, visually differing from the shape of observed data and overestimating the peak concentration of phenol in the reactor. Considering the variability of the system as evident in the range of experimentally determined parameters and solids concentrations over time, the model can be considered successful.

Failure of the two-population model indicated a problem inherent in this model's treatment of two separate populations feeding on the same substrate. Over time, one population or the other became dominant, depending on net growth characteristics. This suggests that other alternatives need to be explored. Possible alternatives include modeling TCE-degradation as a function of oxygenase enzyme level in a single population or modeling TCE degrading organisms as a subset of a larger phenol degrading population.

Parameter Determination

The large variability in solids measurements and k^o values over time may imply that other kinetic parameters also vary over time. Therefore it is necessary to collect many

measurements of kinetic parameters. Some parameters used in this study were not based on large pools of values, and it is possible that deficiencies in modeling were due to inadequate assessments of those parameters.

The sensitivity analysis performed on the model was a powerful tool in determining which parameters are most influential to model predictions. Results of this analysis can guide future research to focus more on the most influential parameters. It was seen that in this model, the yield coefficient played a large role in determining the outcome of all model predictions and future work should reflect this importance.

Recommendations

- The one-population model was shown to adequately predict TCE levels in the reactor. Time required to degrade TCE and phenol concentrations, however were not as accurately modeled. Better estimations of important parameters should be made and the model reevaluated.
- Other two-population models should be explored. Models that consider TCE degradation as a function of enzyme level rather than biomass may have more success and avoid the problems of competition between populations utilizing the same growth substrate.
- Experimental methods of differentiating between forms of biomass need to be developed. Although models can be created to account for dead and decaying cells,

predator populations, heterotrophic bacteria feeding on degradation by-products, etc., experimental verification will not be possible until differential methods are created.

REFERENCES

- Alvarez-Cohen, L. and P. L. McCarty. 1991. "A cometabolic biotransformation model for halogenated aliphatic compounds exhibiting product toxicity." Environ. Sci. Technol. 25: 1381-1387.
- Auteinrieth, R.L., J. S. Bonner, A. Akgerman, and M. Okagun. 1991. "Biodegradation of phenolic wastes." Journal of Hazardous Materials 28: 29-53.
- Beltrame, P., P. L. Beltrame, P. Carniti, and D. Pitea. 1980. "Kinetics of phenol degradation by activated sludge in continuous-stirred reactors." J. Water Pollut. Control Fed. 52: 126-133.
- Chang, H-L. and L. Alvarez-Cohen. 1995a. "Model for the cometabolic biodegradation of chlorinated organics." Environ. Sci. Technol. 29: 2357-2367.
- Chang, H-L. and L. Alvarez-Cohen. 1995b. "Transformation capacities of chlorinated organics by mixed cultures enriched on methane, propane, toluene, or phenol." Biotechnology and Bioengineering 45: 440-449.
- Chang, W-K. 1996. "Kinetics characterization of cometabolizing communities and adaptation to nongrowth substrate." Ph.D. Dissertation.
- Chang, W-K. And C. S. Criddle 1997. "Experimental evaluation of a model for cometabolism: prediction of simultaneous degradation of trichloroethylene and methane by a methanotrophic mixed culture." Biotechnology and Bioengineering 56 (5), 492-501.
- Criddle, C. S. 1993. "The kinetics of cometabolism." Biotechnology and Bioengineering 41: 1048-1056.
- Dabrock, B., J. Riedel, J. Bertram, and G. Gottschalk. 1992. "Isopropylbenze (cumene) - a new substrate for isolation of trichloroethene-degrading bacteria." Archives of Microbiology 158: 9-13.
- Gossett, J. M. 1987. "Measurement of Henry's law constants for C₁ and C₂ chlorinated hydrocarbons." Environ. Sci. Technol. 21: 202-208.
- Henry, S. M. and D. Grbic-Galic. 1990. "Effect of mineral media on trichloroethylene oxidation by aquifer methanotrophs." Microb. Ecol. 10: 151-169.
- Kotturi, G., C. W. Robinson, and W. E. Inniss. 1991. "Phenol degradation by a psychrotrophic strain of *Pseudomonas putida*." Appl. Microbiol. Biotechnol. 34: 539-543.

Metcalf and Eddy, Inc. Tchobangoglous, G. and F. L. Burton. 1991. Wastewater Engineering: Treatment, Disposal and Reuse. 3rd Edition. McGraw-Hill, Inc. New York.

Oldenhuis, R., R. L. J. M. Vink, D. B. Janssen, and B. Witholt. 1989. "Degradation of chlorinated aliphatic hydrocarbons by *Methylosinus trichosporium* OB3b expressing soluble methane monooxygenase." Appl. Environ. Microbiol. 55: 2819-2826.

Segar Jr., R. L., P. Kalia, B. I. Dvorak. 1995 "Simulation of sequencing batch and biofilm reactors for trichloroethylene (TCE) cometabolism." Book: In Situ and On Site Bioremediation: Volume 3.

Shih, Chien-chun. 1995. "Experimental and numerical evaluation of cometabolism in sequencing batch reactors." Ph.D. Dissertation.

Wilson, J. T., and B. H. Wilson. 1985. "Biotransformation of trichloroethylene in soil." Appl. Environ. Microbiol. 29:242-243.

APPENDIX A
MATHCAD PROGRAMMING

The MathCAD model begins with a statement of variables and initial conditions (Figure A-1). Experimentally determined parameters are converted to units of hours for use in the subsequent program. Initial conditions are required by the software to begin the differential equation solving process.

Once initial conditions and parameters have been entered, the next step in MathCAD programming is to enter the differential equations. MathCAD requires these to be entered into a matrix, each row of the matrix corresponding to a different variable. The actual entry is the differential equation. Each variable being solved for is assigned a name based on its position in the differential equation matrix: the first variable, corresponding to the first row of the matrix is named x_0 , the second x_1 , etc. In this program, there are eight rows, corresponding to eight variables. The names of the variables and what they represent are summarized in Table A-1.

Table A-1 MathCAD Variable Legend

Name	Variable
x_0	C_L - Liquid phase TCE concentration (mg/L)
x_1	C_G - Gaseous phase TCE concentration (mg/L)
x_2	V - Reactor liquid volume
x_3	X_{apt} - TCE-degrading biomass concentration (mg/L)
x_4	S - Substrate (phenol) concentration (mg/L)
x_5	$M_{airstrip}$ - Cumulative mass of TCE lost to air stripping (mg)

Each variable has different equations to describe it at different times of the cycle. To deal with this, MathCAD allows conditional statements to be attached to differential equations. Furthermore, conditional statements may be linked by Boolean logic.

Dimensionless Henry's Constant $H = 0.392$
 Airflow into SBR $Q_g = 6 \text{ L/hr}$
 Transformation Capacity $T_{cb} = 0.29 \text{ mgTCE/mg cell}$
 First Order TCE Degradation Coefficient $k = \frac{0.2}{24} \text{ L/mg-hr}$
 Zero-order Phenol Degradation Coefficient $k_p = \frac{2.6}{24} \text{ 1/hr}$
 Endogenous Decay $b = \frac{0.05}{24} \text{ 1/hr}$
 Yield on Phenol $Y = 1.3 \text{ mg/mg}$

Initial Conditions

Reactor Volume $V_o = 1.25 \text{ L}$
 TCE concentration injected $C_o = 5 \text{ mg/L}$
 Phenol concentration injected $P_o = 7200 \text{ mg/L}$
 Total Reactor Volume $V_t = 2.5 \text{ L}$
 Initial Biomass $X_{ato} = 2000 \text{ mg/L}$
 Initial Reactor Concentration $C_{Lo} = 0 \text{ mg/L}$
 Initial Gaseous Phase Concentration $C_{Go} = 0$
 Initial Liquid Volume $V_{lo} = 1.25 \text{ L}$
 Initial Phenol Concentration in Reactor $P_{Lo} = 0$

a = 1 A coefficient was added to the mass transfer term to investigate the effects of a change in the mass transfer coefficient (not used in this study)

Figure A-1 MathCAD Programming Worksheet

$$\begin{aligned}
 & \left[\begin{array}{l} 1.00 - Co \cdot x_0 \\ Vlo - t \cdot 1.00 \end{array} \right] \cdot 1.73892 \cdot a \cdot x_2 \cdot \left[\begin{array}{l} 1.28922 \cdot x_0 \\ x_0 \end{array} \right] \cdot \frac{x_1}{H} \cdot (k) \cdot x_0 \cdot x_3 \quad \text{if } 0 \leq t \leq 1 \\
 & \left[\begin{array}{l} 1.73892 \cdot a \cdot x_2 \\ 1.28922 \cdot x_0 \end{array} \right] \cdot \frac{x_1}{H} \cdot k \cdot x_0 \cdot x_3 \quad \text{if } 1 < t \leq 4 \\
 & 0 \quad \text{if } x_0 < 0 \\
 & 0 \quad \text{otherwise}
 \end{aligned}$$

$$\begin{aligned}
 & \left[\begin{array}{l} 1.73892 \cdot a \cdot x_2 \\ 1.28922 \cdot x_0 \end{array} \right] \cdot \frac{x_2}{Vt - x_2} \cdot \left(x_0 \cdot \frac{x_1}{H} \right) - Qg \cdot \frac{x_1}{Vt - x_2} - \frac{x_1 \cdot 1.00}{Vt \cdot x_2} \quad \text{if } 0 \leq t \leq 1 \\
 & \left[\begin{array}{l} 1.73892 \cdot a \cdot x_2 \\ 1.28922 \cdot x_0 \end{array} \right] \cdot \frac{x_2}{Vt - x_2} \cdot \left(x_0 \cdot \frac{x_1}{H} \right) - Qg \cdot \frac{x_1}{Vt - x_2} \quad \text{if } 1 < t \leq 4 \\
 & 0 \quad \text{if } x_1 < 0 \\
 & 0 \quad \text{otherwise}
 \end{aligned}$$

$$\begin{aligned}
 & 1.00 \quad \text{if } 0 \leq t \leq 1 \\
 & (-1.00) \quad \text{if } 5 < t \leq 6 \\
 & 0.05 \quad \text{if } 6 \leq t \leq 6.5 \\
 & 0 \quad \text{otherwise}
 \end{aligned}$$

$$\begin{aligned}
 & \left[\begin{array}{l} x_3 \\ Vlo - t \cdot 1.00 \end{array} \right] \cdot \frac{k \cdot (x_0)}{Tcb \cdot k \cdot x_0 \cdot x_3} \cdot x_3 \cdot b \cdot x_3 \quad \text{if } 0 \leq t \leq 1 \\
 & \left[\begin{array}{l} b \cdot x_3 \\ \frac{k \cdot (x_0)}{Tcb \cdot k \cdot x_0 \cdot x_3} \end{array} \right] \cdot x_3 \quad \text{if } 1 < t \leq 4 \\
 & b \cdot x_3 \quad \text{if } 4 < t \leq 5 \\
 & b \cdot x_3 \cdot \frac{x_3}{x_2} \cdot (-1.00) \quad \text{if } 5 < t \leq 6 \\
 & \left[\begin{array}{l} x_3 \\ Vlo - (t - 6) \cdot 0.05 \end{array} \right] + Y \cdot kp \cdot x_3 \quad \text{if } (6 < t \leq 6.5) \cdot (x_4 > 0) \\
 & \left[\begin{array}{l} x_3 \\ Vlo - (t - 6) \cdot 0.05 \end{array} \right] + b \cdot x_3 \quad \text{if } (6 < t \leq 6.5) \cdot (x_4 < 0) \\
 & Y \cdot kp \cdot x_3 \quad \text{if } (6.5 < t \leq 12) \cdot (x_4 > 0) \\
 & -b \cdot x_3 \quad \text{if } (6.5 < t \leq 12) \cdot (x_4 < 0) \\
 & 0 \quad \text{otherwise} \\
 & \left[\begin{array}{l} 0.05 \\ Vo - 0.05 \cdot (t - 6) \end{array} \right] \cdot (Po - x_4) \cdot kp \cdot (x_3) \quad \text{if } (6 < t \leq 6.5) \cdot (x_4 > 0) \\
 & \left[\begin{array}{l} 0.05 \\ Vo - 0.05 \cdot (t - 6) \end{array} \right] \cdot (Po) \quad \text{if } (6 < t \leq 6.5) \cdot (x_4 < 0) \\
 & kp \cdot (x_3) \quad \text{if } ((6.5 < t \leq 12)) \cdot (x_4 > 0) \\
 & 0 \quad \text{if } (6.5 < t \leq 12) \cdot (x_4 < 0) \\
 & 0 \quad \text{otherwise}
 \end{aligned}$$

$$Qg \cdot x_1$$

$$1$$

Figure A-2 MathCAD Equation Matrix (One-population model)

A program is created to evaluate the differential equations repeatedly, changing the initial conditions for biomass concentration with each iteration. Solutions are placed in a matrix. Figure A-3 contains the program used in this work.

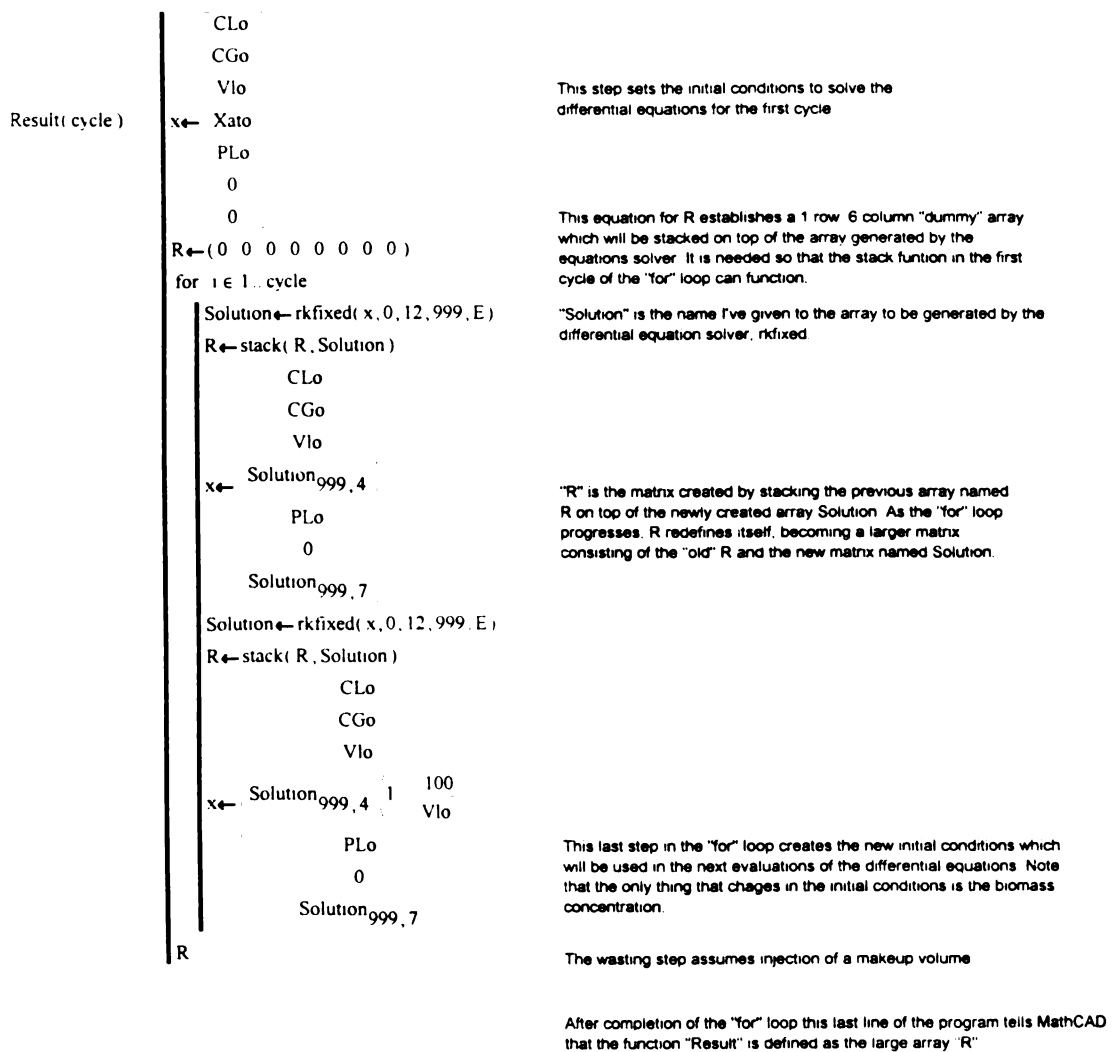


Figure A-3 MathCAD Program

Evaluation of the program requires the input of the number of days to be modeled. Output can be in the form of a matrix or by graphing explicit columns of the solution matrix.

APPENDIX B
MASS TRANSFER COEFFICIENT DETERMINATION

The mass transfer coefficient was determined by spiking a known mass of TCE into the reactor at various volumes prior to inoculation with microorganisms and measuring the presence of TCE in the reactor headspace over time. From this data a mass transfer coefficient was determined at each volume. This data was plotted versus volume and a best fit analysis was performed using Microsoft Excel software. The plot with determined equation and r^2 value is presented in Figure B-1.

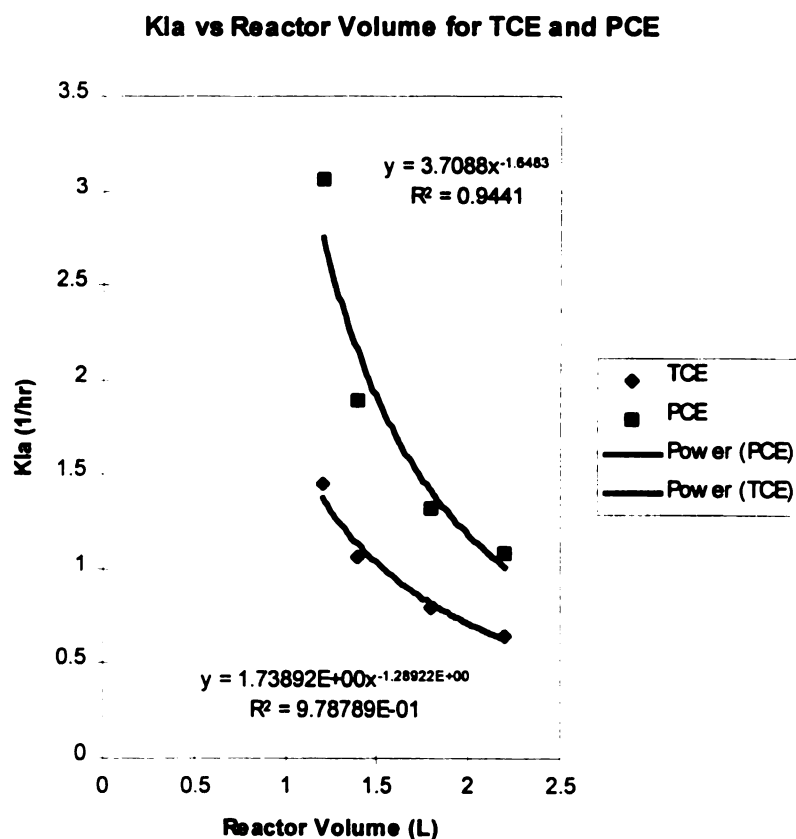


Figure B-1 Mass Transfer Coefficient Relationship